united nations
educational, scientific
and cultural
organization

international atomic
energy agency

the
abdus salam
international centre for theoretical physics

40th anniversary
1964
2004

H4.SMR/1586-1

**"7th Workshop on Three-Dimensional Modelling
of Seismic Waves Generation and their Propagation"**

25 October - 5 November 2004

Theoretical and Oberved Envelopes of Scattered High Frequency Seismic Waves at Local to Regional Distance

A. Gusev

Institute of Volcanology & Seismology
Russian Academy of Sciences
Petropavlovsk-Kamchatsky, Russia

A.A.Gusev

Theoretical and observed envelopes of scattered high-frequency seismic waves at local to regional distances

OUTLINE:

1. RANDOM MEDIA, RANDOM AND OBSERVED SIGNAL
2. MORPHOLOGY OF SCATTERED WAVES ON THE EARTH. CODA
3. THEORY. RANDOM SCATTERERS, RANDOM INHOMOGENEITY
4. SIMULATED ENVELOPES
5. INVERSION FOR TURBIDITY
6. NON-UNIFORMITY OF SCATTERER DENSITY IN THE EARTH

Common models of the medium where the waves propagate

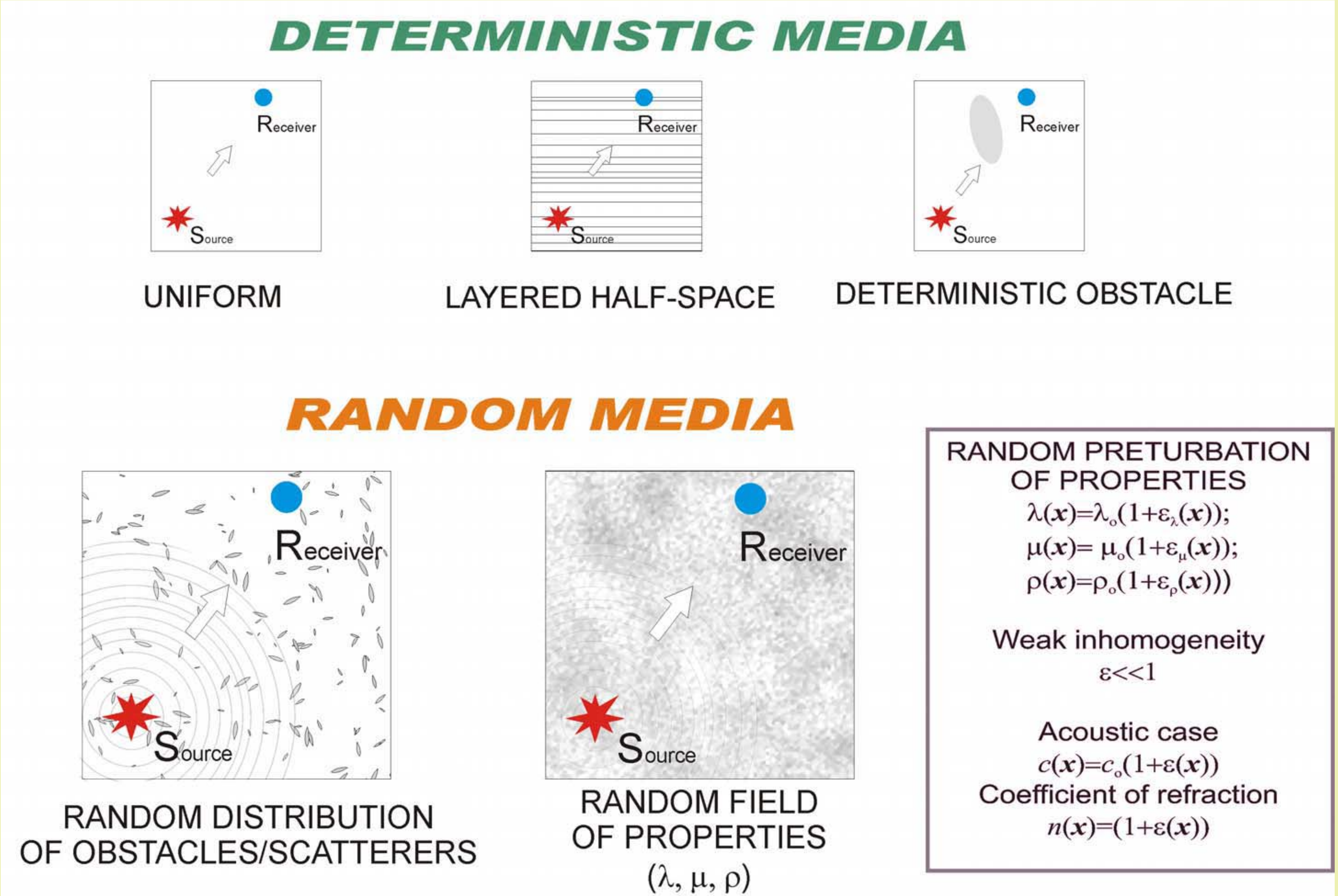

Random-like real-Earth structures

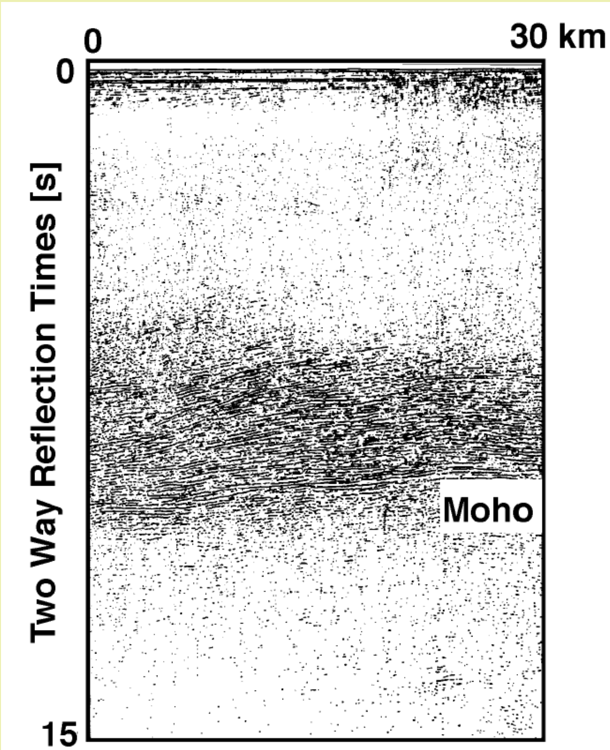

Example reflection-seismic section: strong heterogeneity in the lower crust **(Warner, 1990)**

anisotropic
non-uniform
random field

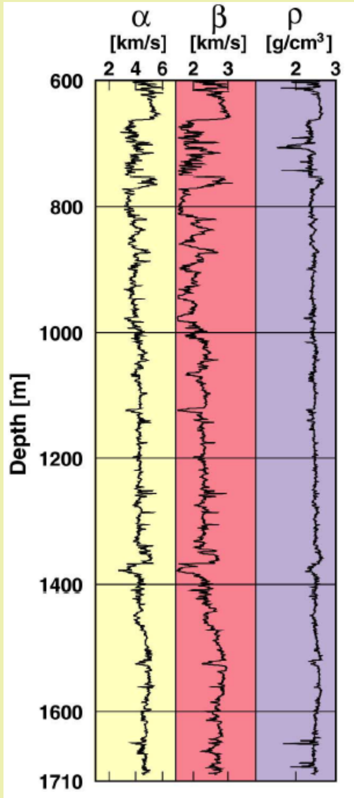

Example well log Persistent oscillation of elastic parameters **(Shiomi et al.,1997)**

non-Gaussian
random field

RANDOM INHOMOGENEITY OR PERTURBATION OF PROPERTIES:

$\lambda(\boldsymbol{x})=\lambda_o(1+\varepsilon_\lambda(\boldsymbol{x}))$;
$\mu(\boldsymbol{x})=\mu_o(1+\varepsilon_\mu(\boldsymbol{x}))$;
$\rho(\boldsymbol{x})=\rho_o(1+\varepsilon_\rho(\boldsymbol{x}))$;

Background: λ_o , μ_o , ρ_o
Perturbation: $\varepsilon_\lambda(\boldsymbol{x})$, $\varepsilon_\mu(\boldsymbol{x})$, $\varepsilon_\rho(\boldsymbol{x})$

Acoustic case: $c(\boldsymbol{x})=c_o(1+\varepsilon(\boldsymbol{x}))$;

Usual assumptions w.r.t. perturbation field:

(1) Weak: $\varepsilon(\boldsymbol{x}) << 1$

(2) Uniform = homogeneous = statationary:

$$\mathrm{Cov}(\varepsilon(\boldsymbol{x}), \varepsilon(\boldsymbol{x}+\boldsymbol{y})) = \sigma_\varepsilon^2\rho(\boldsymbol{y})$$

(3) Isotropic: $\rho(\boldsymbol{y}) \rightarrow \rho(||\boldsymbol{y}||) = \rho(r)$

(in the non-Gaussian case,

more detals are needed)

Random signal, envelope, power (1)

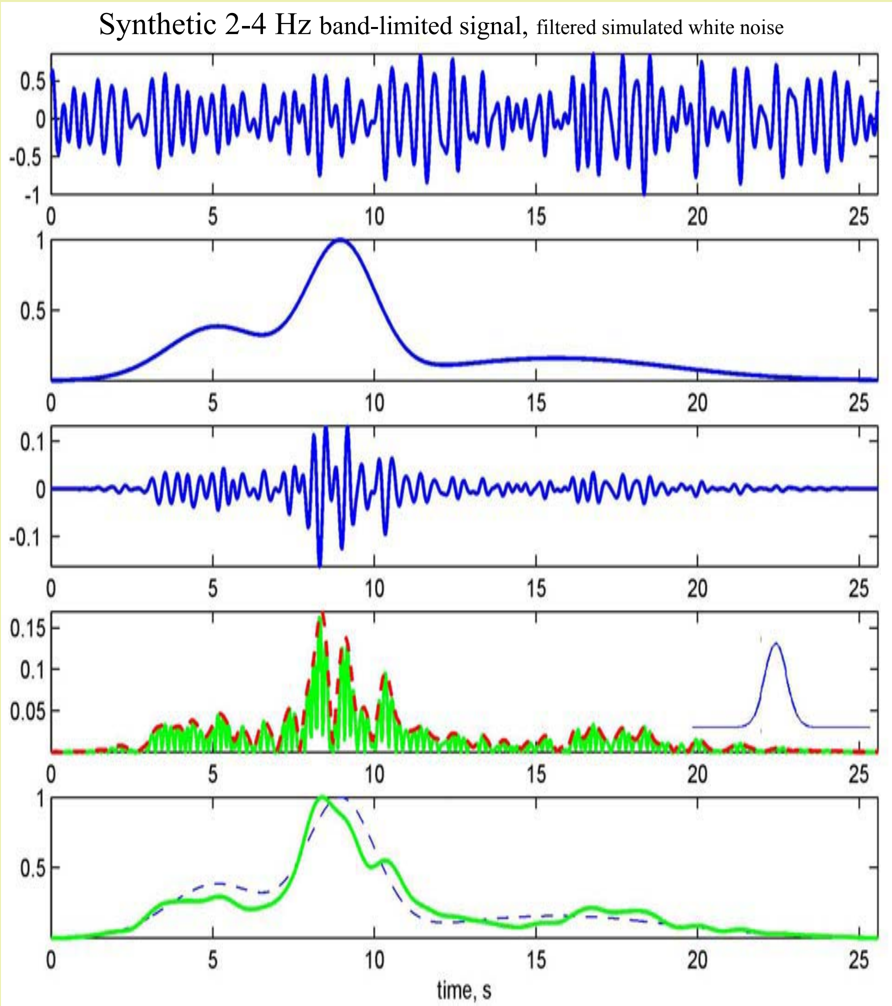

— **stationary random signal *x(t)***

constant mean power or variance: $\sigma^2(t)=\langle x^2(t)\rangle$
constant"true"rms amplimude: $a_{rms}(t)\equiv\sigma(t)$

— **"true" envelope or modulating function *a(t)***
($a^2(t)$ - "True" power time history)

— **$y(t)=x(t)\times a(t)$: simulates observed QUASIstationary signal,**

— **abs (*y(t)*)**
------ **module of analytic signal (MAS)**

— **$a_e(t)$ = SQRT(smoothed $y^2(t)$)**
------- ***a(t)***

$a_e(t)$: empirical envelope,
an estimate for "true" *a(t),*
like those derived from data
$a_e^2(t)$: observed time history
for power
$a_e(t)$ can be also estimated using signal peaks

"True": pertains to ENSEMBLE AVERAGE or MEAN of the process
"Observed": pertains to a single SAMPLE FUNCTION or
a REALIZATION of the random process

Random signal, envelope, power (2)

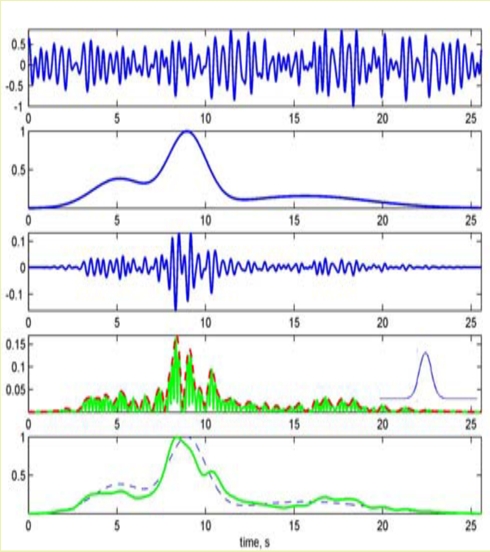

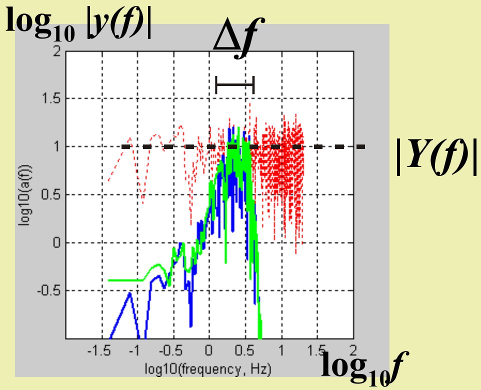

3. Denote $P(f\,|t)$ signal power spectrum, average over a window of length d around t

Then

$P(f\,|t)= 2|y(f)|^2 /d$

1. Main signal parameters:

f_c – central frequency of a band

Δf – bandwidth (1/ Δf - time scale of "instant" power change)

$t_{drift} \approx \max(a(t))(da(t)/dt)^{-1}$
– time scale of non-stationarity

T_{sm} – width of smoothing window

Condition of quasi-stationarity:

$t_{drift} >> 1/\Delta f$

Condition on smoothing window:

$T_{sm} >> 1/\Delta f$

2. Denote:

$|Y(f)|$ – Fourier amplitude spectral level, average over the bandwidth Δf

d – signal duration (or window duration)

y_{rms} – rms signal amplitude over d

Then (Parseval's theorem):

$$2\,|Y(f)|^2\,\Delta f = y_{rms}^{\ 2} d$$

[permits to convert time domain to spectral domain estimates and back]

Regional seismograms – examples, morphology

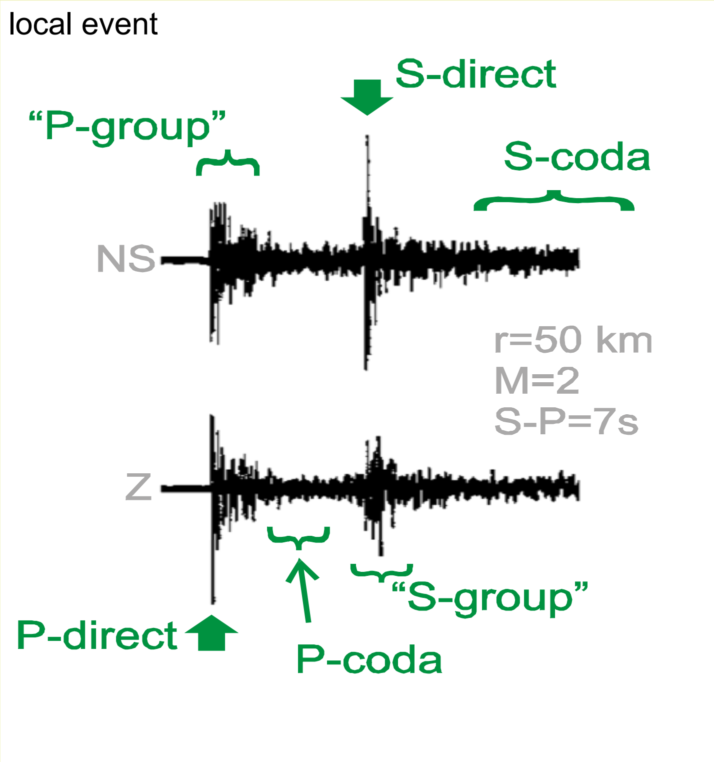

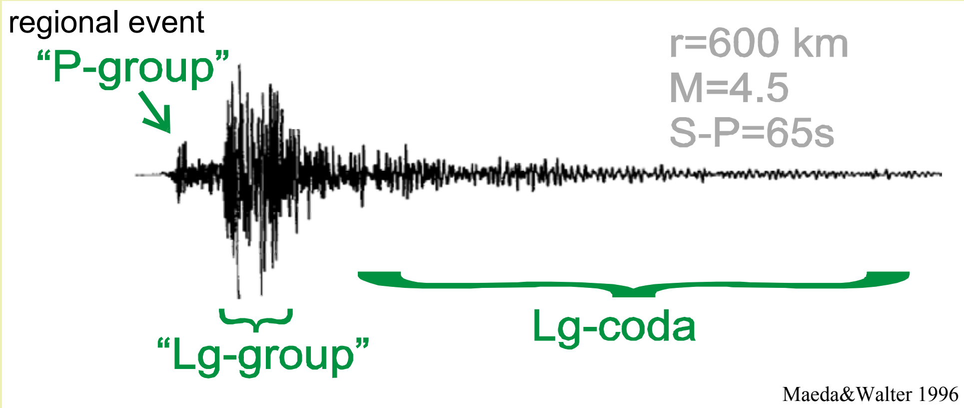

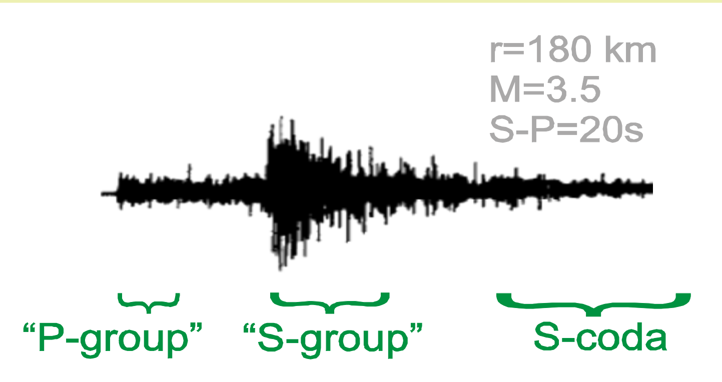

P-direct, S-direct – represent source-time-function, disappear at *r*=15-70 km for shallow events, short spikes for low magnitudes

P-group – appearance defined by medium, mix of P-direct, P-P forward scattered and P-S converted

P-coda – P-P wide-angle scattered and P-S converted

S/Lg-group – mix of S and HF surface waves, direct and forward-scattered

S/Lg-coda – S and HF surface waves, wide-angle scattered

Regional envelopes

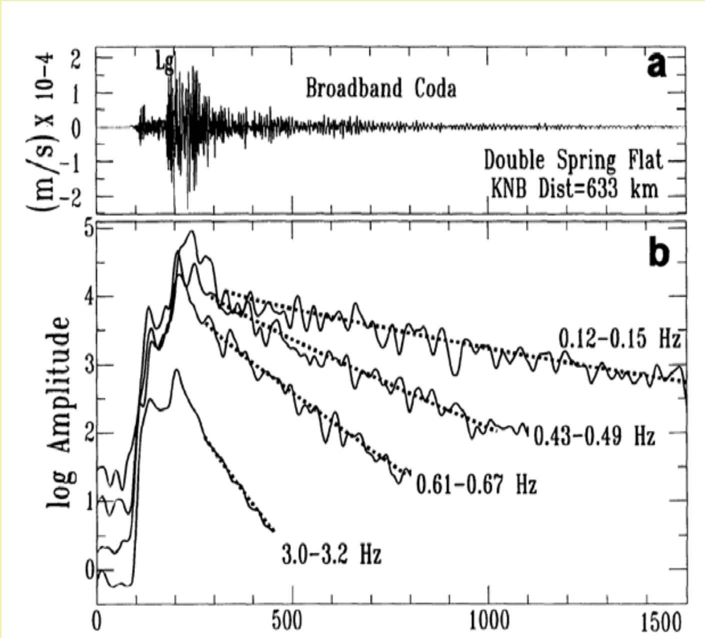

Maeda&Walter 1996

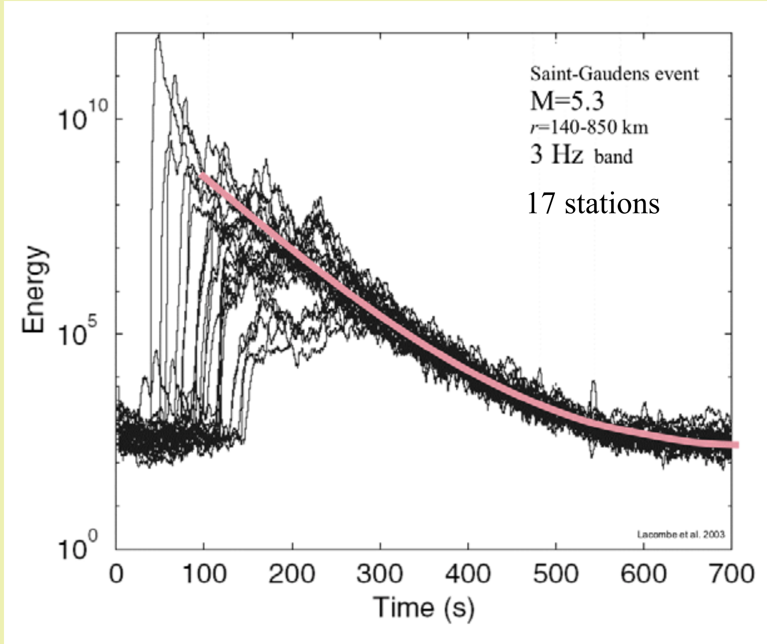

1. Envelopes from band-filtered HF records show systematic structure, first of all coda
2. To select coda, use sufficient delay, like $2t_S$ (*coda window*)
3. Coda decay is monotonous, regular, frequency dependent
4. Coda envelope is approximately station-independent
   (a certain constant factor is present, it depends on local geology, useful for site specification)

Regional coda

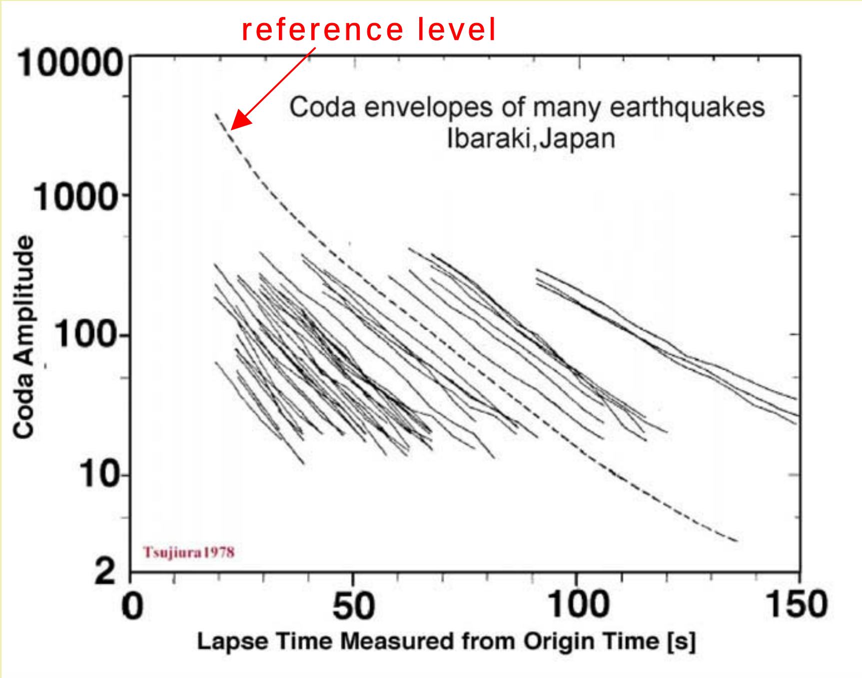

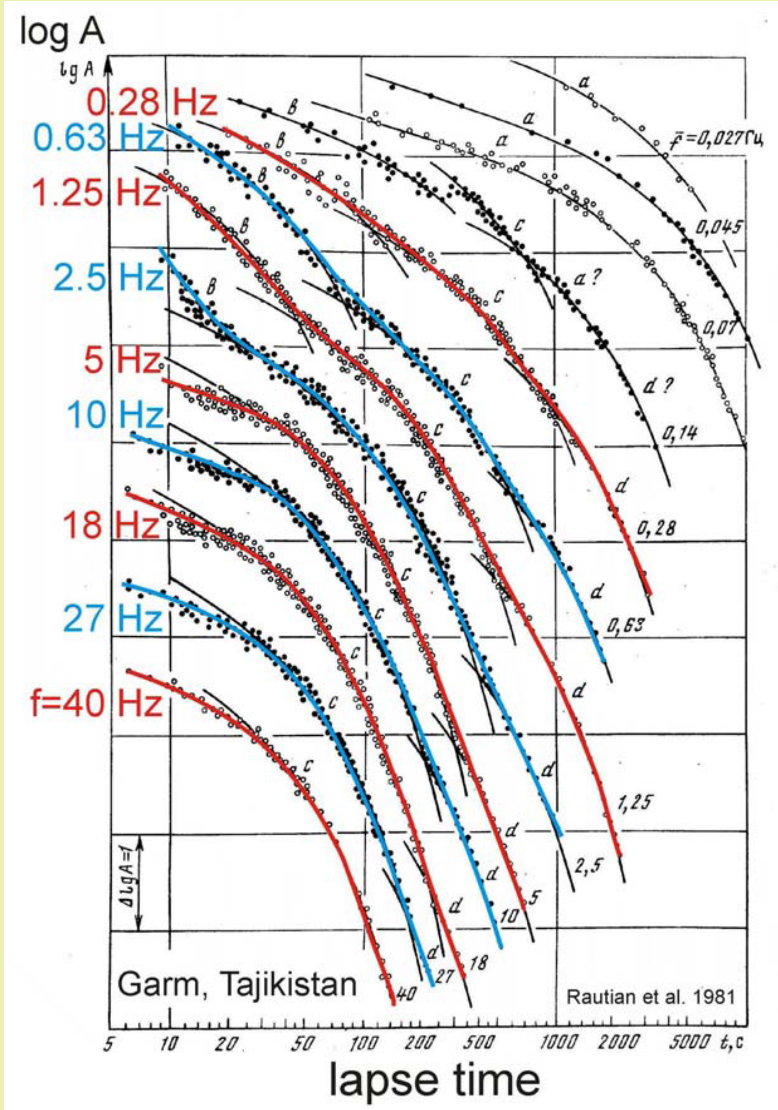

1. Coda envelope *shape* is approximately event-independent.

2. The scaling factor to reduce observed coda amplitude to a reference level gives (*f*-dependent) coda magnitude. After additional calibration it gives source spectrum $M_0(f)$

Temporal variations of coda shape and level

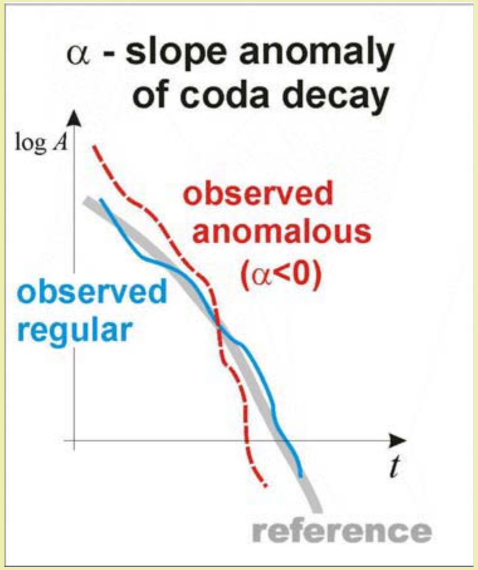

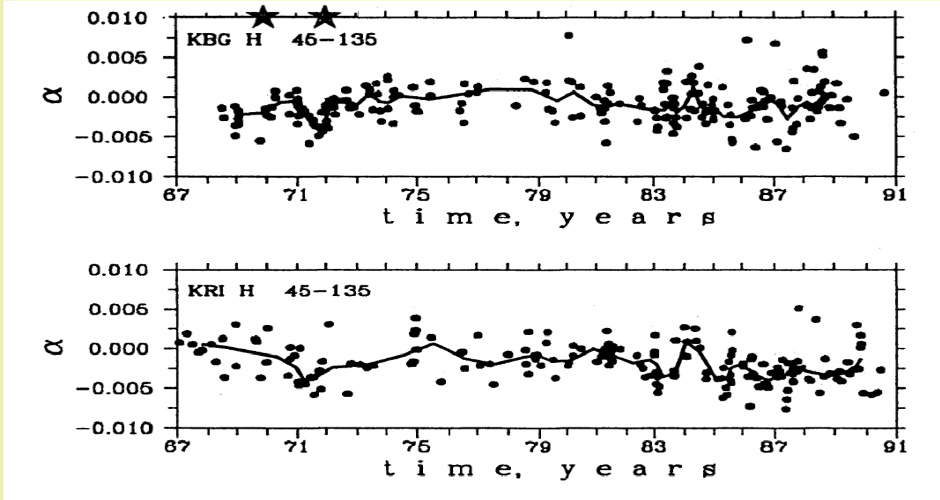

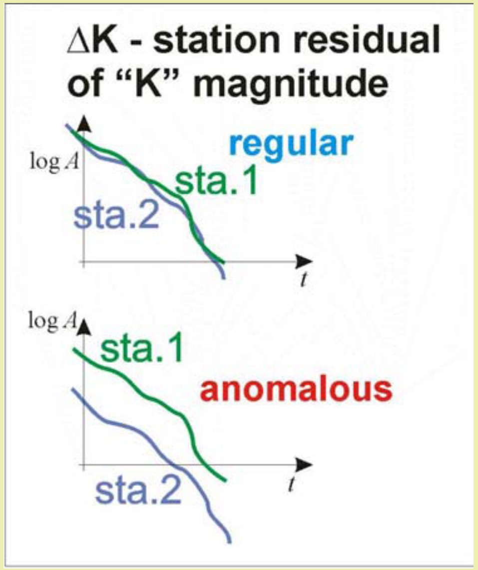

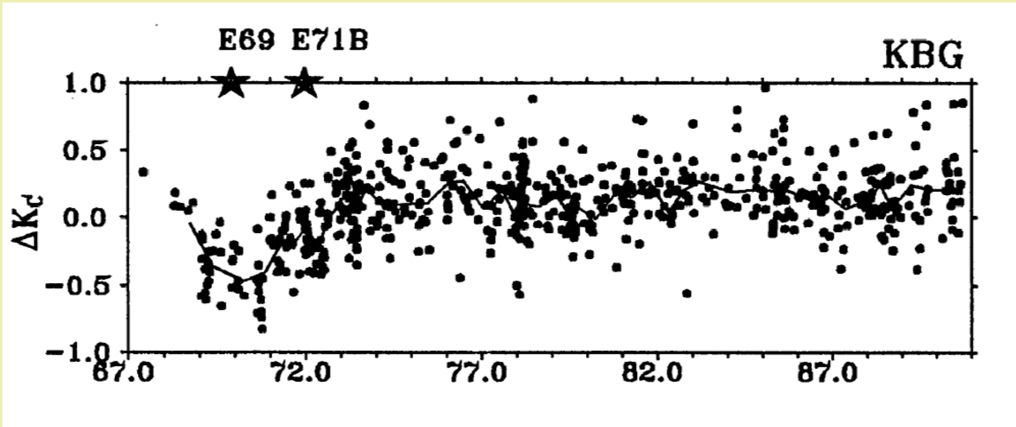

Coda magnitudes. Source spectra from coda

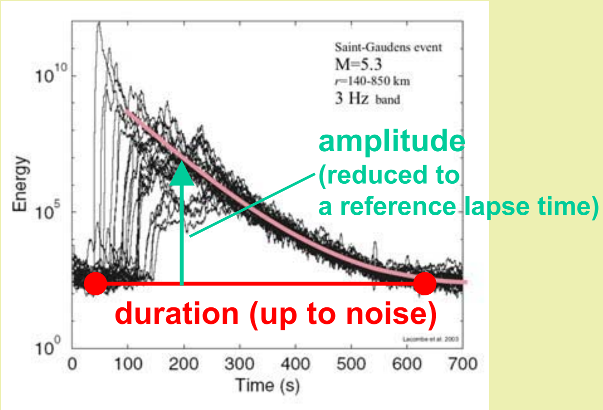

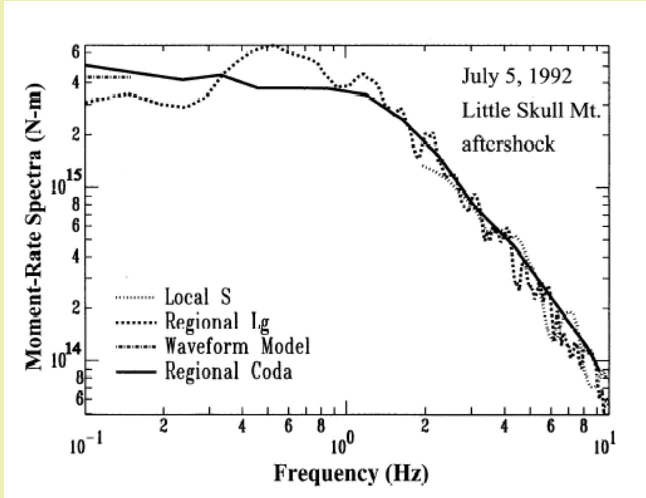

Maeda&Walter 1996

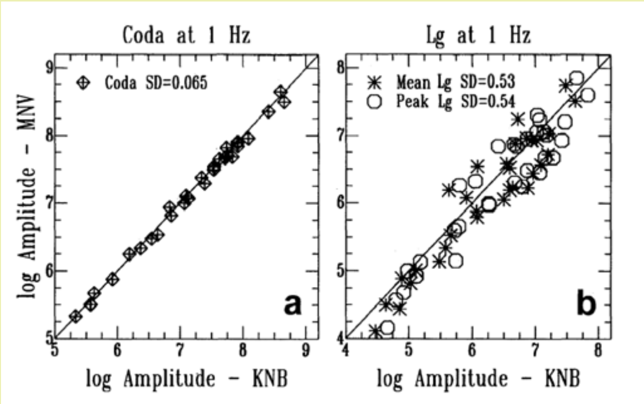

Maeda&Walter 1996

a set of coda magnitudes can be converted to an accurate source spectrum $\dot{M}_0(f)$

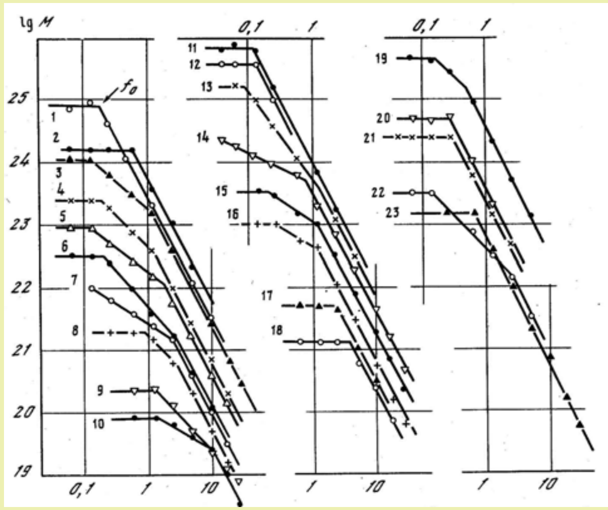

Rautian et al. 1981

amplitude-based coda magnitude provides unsurpassed intrinsic accuracy: σ(single $\log_{10}$A measurement)=0.05-0.1, against 0.2-0.4 for usual magnitudes

Regional envelopes – body wave pulses

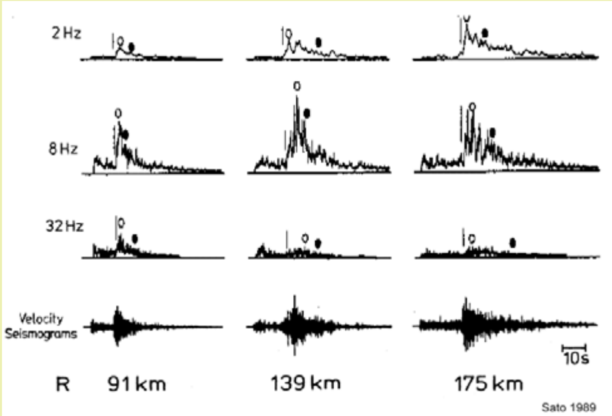

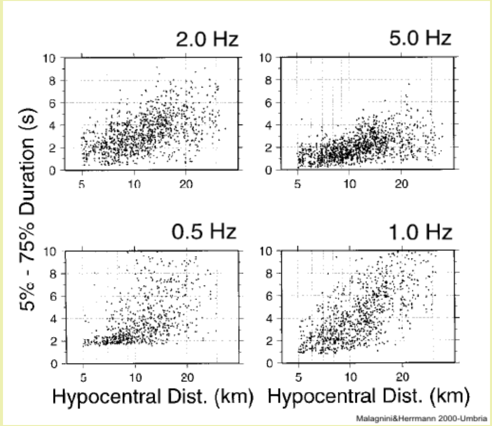

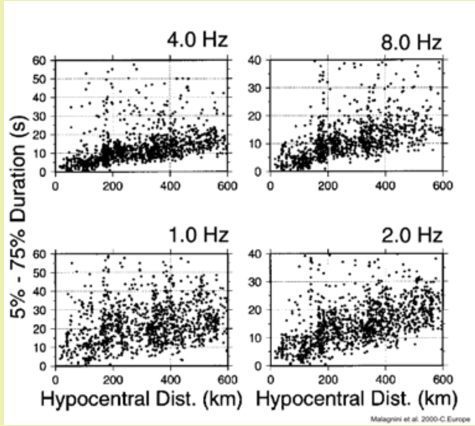

1. The duration of a body-wave group is difficult to parametrize and measure because of a very heavy coda tail. Different definitions can be based on:
   - ideally – mean delay of energy; in practice: onset-to-centroid or onset-to-peak time,
   - ideally - rms width of energy distribution, in practice: rms duration ("standard deviation") of truncated data, or "interquantile range" of energy distribution in time, like 5%-75% range.

2. The duration of a body-wave group grows with hypocentral distance in the local (0-100km) and regional (0-600km) distance ranges. Pulse broadening is seen for oblique, near-horizintal and near-vertical rays. Lg over continental paths behaves differently, with saturation of duration.

Regional envelopes as a whole

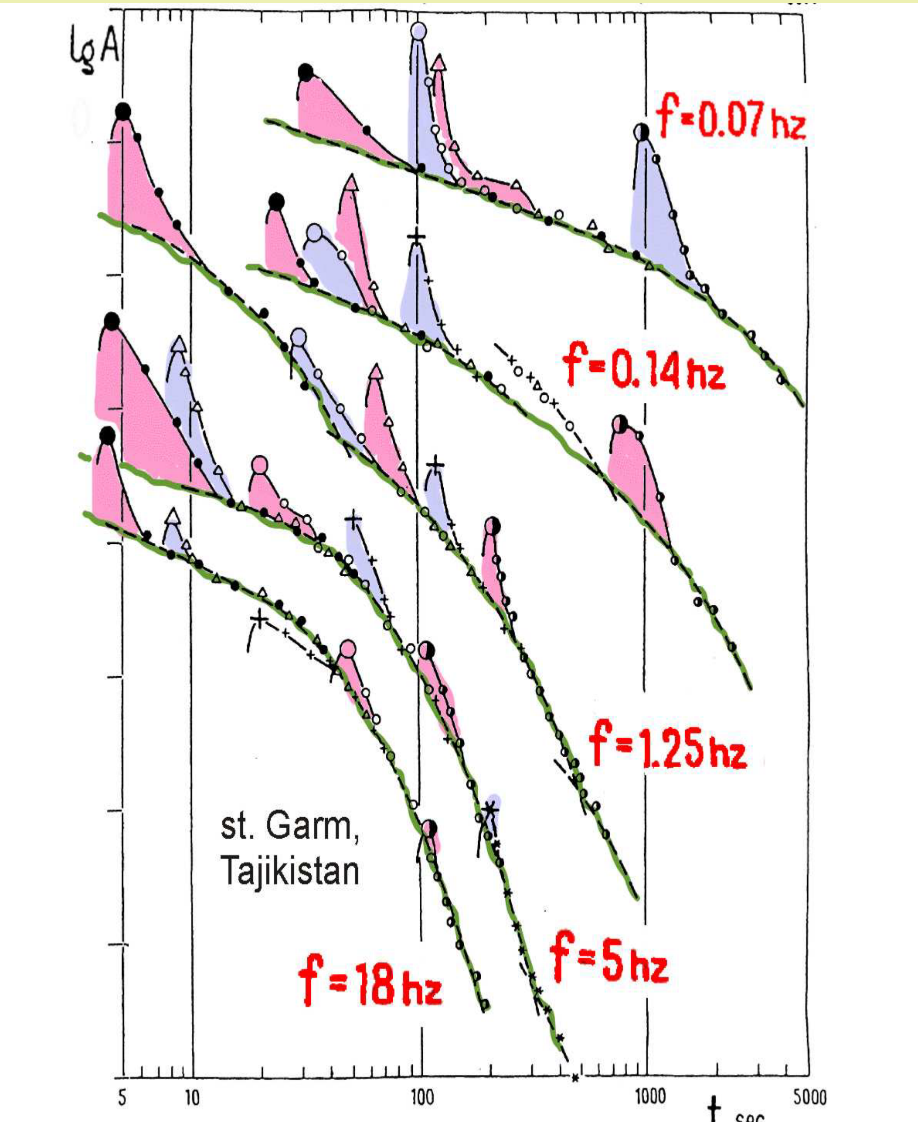

Rautian et al. 1981

Over 20-30 to 500-1000 km distance range, S-wave group of increasing, medium-related duration is seen.

Typically S wave amplitudes are *above* coda asymptote.

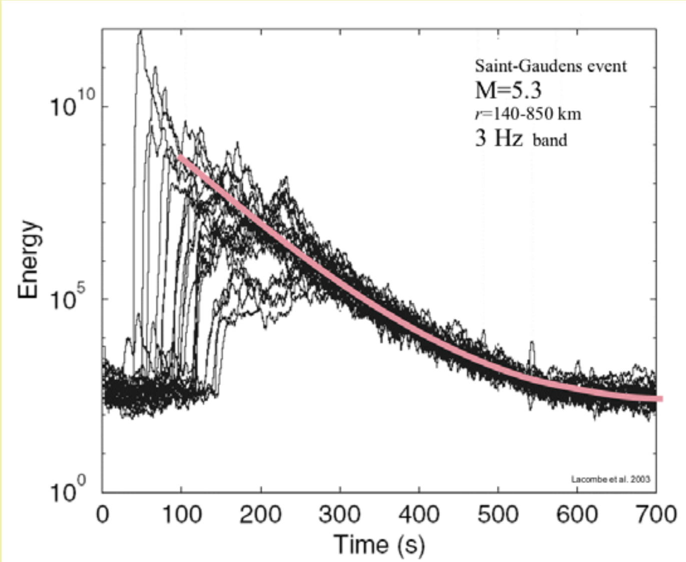

Diffusive envelopes – lunar, volcanic

lunar seismograms

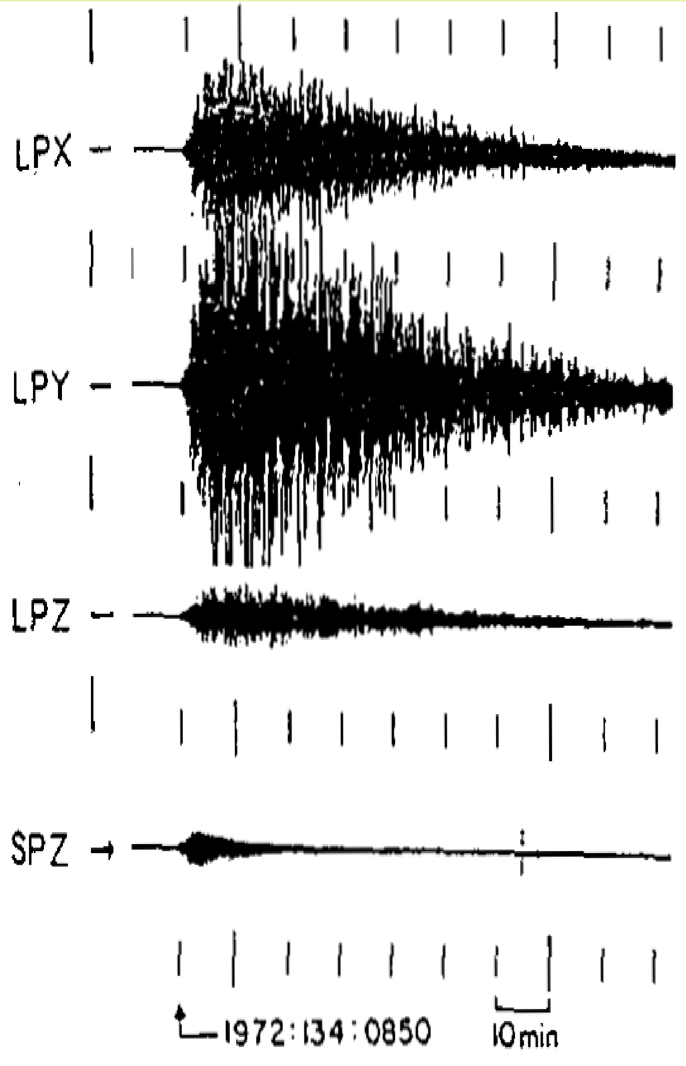

B-type event on Merapi volcano

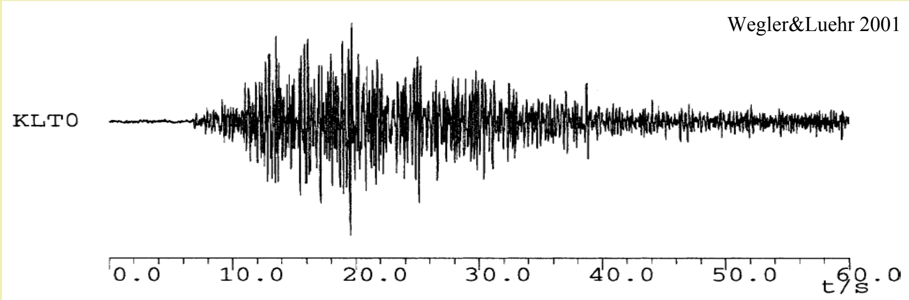

Spindle-like envelopes are characteristic for lunar seismograms and also for shallow events near volcanos ("Minakami B-type events").

One sees very emergent onset, no direct body wave, no indications of S wave group. Coda is clear and stable.

Such a picture is associated with wave energy diffusion in the medium (relatively very strong scattering).

(Contribution of source duration negligible)

Theory. Scattering coefficient or turbidity

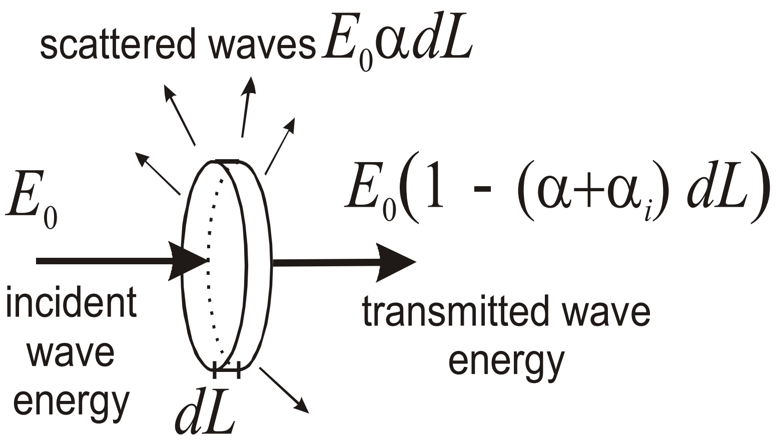

integrating loss along incident ray:

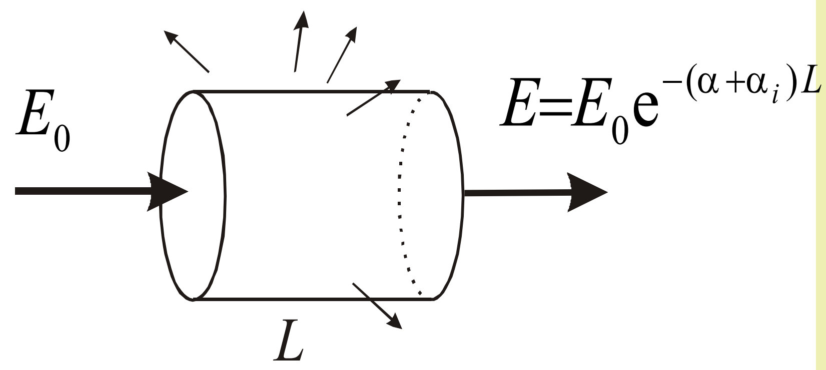

α - scattering coefficient or turbidity (also α_s, also g)
fractional loss of energy to scattering, per 1 km
probability of scattering per 1 km
units: km^{-1}

α_i - absorption coefficient
fractional intrinsic/inelastic loss, per 1 km

$\alpha_t = \alpha+\alpha_i$ - attenuation/extinction coefficient
fractional *total* loss, per 1 km

Dimensionless quality factors Q are defined:
Q^{-1} = fractional loss per (wavelength/2π)
so that

$\alpha_s = 2\pi f/cQ_s \quad \alpha_i = 2\pi f/cQ_i \quad \alpha_t = 2\pi f/cQ_t$

and: $1/Q_t = 1/Q_s + 1/Q_i$

for a beam of particles:
α is the probability of scattering per 1 km;
hence:
Mean Free Path: $l = 1/\alpha$ [km]

Angular distribution of scattered energy. Phase function or indicatrix (1)

$$\alpha = \int_{\Omega} \alpha_{diff}(\Omega)\, d\Omega$$

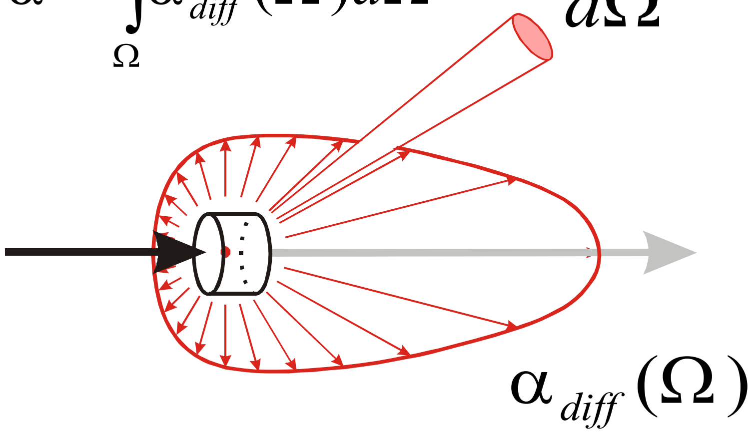

$\alpha_{diff}(\Omega)$ - differential scattering coefficient,
fractional scattering loss
per km per unit solid angle
(per steradian)

$\phi(\Omega)=\alpha_{diff}(\Omega)/\alpha$ - indicatrix or phase function

$$1 = \int_{\Omega} \phi(\Omega)\, d\Omega$$

$\phi(\Omega)$ can be treated as probability density
for a scattered particle to select a particular position
on a distant sphere around the scattering subvolume

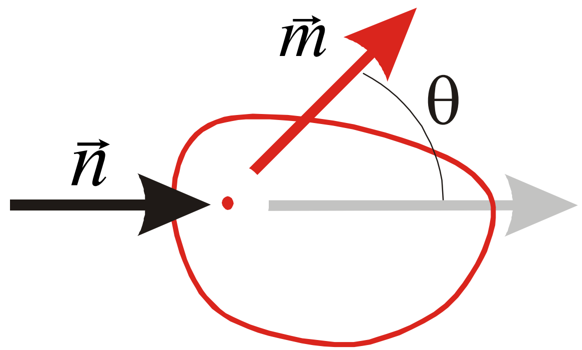

general case,

$$\phi() = \phi(\Omega_n, \Omega_m) \Rightarrow \phi(\vec{n}, \vec{m})$$

scattering angle :

$$\theta = \arccos(\vec{m} \cdot \vec{n})$$

Phase function (continued)

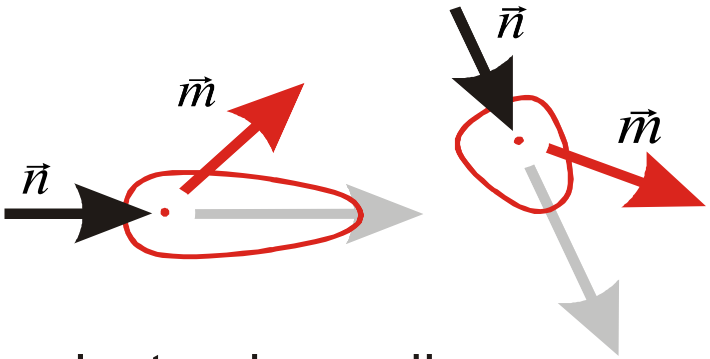

anisotropic-medium case
(anisotropic w.r.t. N-E-Z reference,
seems adequate e.g. for layered crust)

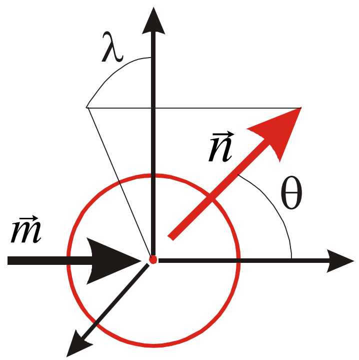

$$\phi(\vec{m},\vec{n}) = const = \frac{1}{4\pi}$$

isotropic-medium and ray-isotropic case
the simplest case

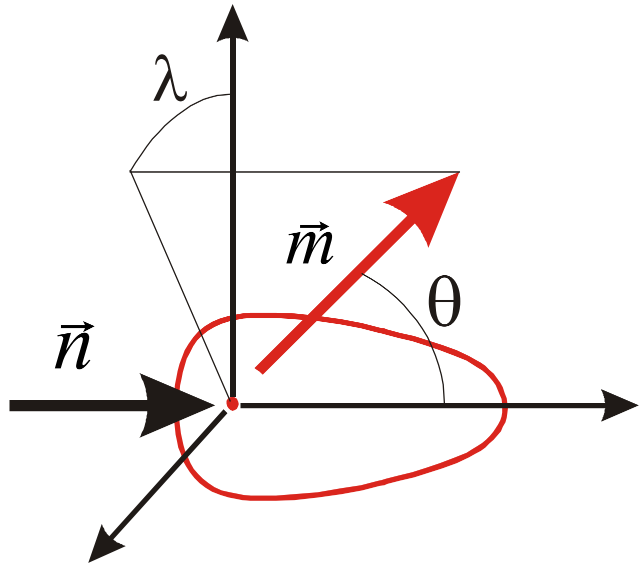

$$\phi(\vec{n},\vec{m}) \Rightarrow \phi(\cos(\vec{n},\vec{m})) \Rightarrow \phi(\theta)$$

non-isotropic,
or anisotropic
("ray-anisotropic")
case, axisymmetrical
("isotropic-medium" case, with statistically isotropic medium;
no isotropy w.r.t. incident ray direction)

Equations of radiative transfer (stationary case)

Define $I_s(\boldsymbol{r},\boldsymbol{n})$
- scattered radiation intensity at $\boldsymbol{r}$ along $\boldsymbol{n}$ as: $dP_s = I_s(\boldsymbol{r},\boldsymbol{n})\, d\Omega_n$
where dP_s is scattered wave power propagating from $\boldsymbol{r}$, along $\boldsymbol{n}$, into a cone with a solid angle $d\Omega_n$

Similarly, define $I_0(\boldsymbol{r},\boldsymbol{n})$
- direct ("ballistic") radiation intensity at $\boldsymbol{r}$ along $\boldsymbol{n}$ (from a certain source).
For the case of a point source, assume that a ray from it is along $\boldsymbol{n}$ at $\boldsymbol{r}$.

(all this with respect to radiation in a certain frequency band Δf)

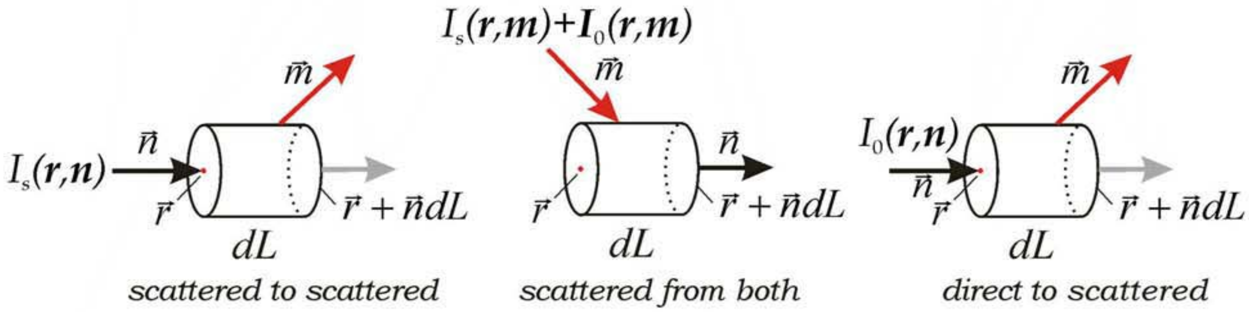

$I_s(\boldsymbol{r}+\boldsymbol{n}dl,\ \boldsymbol{n}) - I_s(\boldsymbol{r},\boldsymbol{n}) = -dI_1 + dI_2 = \text{(loss)}+\text{(gain)}$

loss: $dI_1 = \alpha I_s(\boldsymbol{r},\boldsymbol{n})dL + \alpha_i I_s(\boldsymbol{r},\boldsymbol{n})dL$ [scatt.+intr.],

(here α is the sum over all $\boldsymbol{m}$!)

gain: $$dI_2 = \alpha \int_{4\pi} \left(I_s(r,\boldsymbol{m}) + I_0(r,\boldsymbol{m})\right)\phi(\boldsymbol{m},\boldsymbol{n})d\Omega_m$$

and similarly for I_0, giving:

$$\frac{dI_s(\boldsymbol{r},\boldsymbol{n})}{dL} = -\alpha I_s(\boldsymbol{r},\boldsymbol{n}) - \alpha_i I_s(\boldsymbol{r},\boldsymbol{n}) + \alpha \int_{4\pi} \left(I_s(\boldsymbol{r},\boldsymbol{m}) + I_0(\boldsymbol{r},\boldsymbol{m})\right)\phi(\boldsymbol{m},\boldsymbol{n})d\Omega_m$$

$$\frac{dI_0(\boldsymbol{r},\boldsymbol{n})}{dL} = -\alpha I_0(\boldsymbol{r},\boldsymbol{n}) - \alpha_i I_0(\boldsymbol{r},\boldsymbol{n})$$

$\left(\text{in the non-stationary case, use } I_s = I_s(\boldsymbol{r},t,\boldsymbol{n}), \text{ and } \frac{\mathrm{d}}{\mathrm{d}L} = \boldsymbol{n}\nabla + \frac{1}{c}\frac{\partial}{\partial t} \text{ instead of } \frac{d}{dL}\right)$

Isotropic scattering case: general

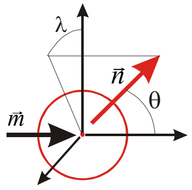

$\phi(\vec{m},\vec{n}) = const = \frac{1}{4\pi}$

isotropic-medium and ray-isotropic case
the simplest case

consider the simplest case:

- **instant point source flashing at *t*=0,**
- **unit source energy in the frequency band (*f*-Δ*f*, *f*+Δ*f*);**
- **acoustic/scalar waves: no conversion, no polarization**
- **isortopic scattering**

DEFINITIONS

basic parameters:

r	source to receiver distance;
c	body wave speed (in applications, mostly S-wave speed);
f, Δf	wave frequency and bandwidth; $\omega = 2\pi f$
$\lambda = c/f$	wavelength
$k = 2\pi/\lambda = \omega/c$	wavenumber
$P(r, t)$	wave intensity in the same band (omnidirectional);
$P_c(t)$	coda intensity: $P(r, t) \rightarrow P_c(t)$ when $t \gg r/c$
l	mean free path
$t^* = l/c$,	mean free time
Q	quality factor due to scattering ($Q = \omega t^*$)

***dimensionless / scaled parameters*:**

$\rho \equiv r/l$	scaled distance
$\tau \equiv cr/l = t/t^*$	scaled lapse time
$i(\rho, \tau)$, $i_c(\tau)$	scaled scattered intensity (3D, use l^2 for 2D):

$$i(\rho,\tau) = \left(l^3/c\right) P(r,t)$$

$i_c(\tau) \equiv i(0,\tau)$	scaled coda intensity:

OMNIDIRECTIONAL WAVE INTENSITY

$$P_s(\boldsymbol{r},t) = \int_{4\pi} I_s(\boldsymbol{r},t,\boldsymbol{n})\,d\Omega_n \qquad \text{scattered}$$

$$P(\boldsymbol{r},t) = \int_{4\pi} \left(I_0(\boldsymbol{r},t,\boldsymbol{n}) + I_s(\boldsymbol{r},t,\boldsymbol{n})\right) d\Omega_n \qquad \text{total}$$

Isotropic scattering case: SIS

ρ« 1, τ « 1

Single (isotropic) scattering model - SIS

(single= Born approximation):,

$$i^{SIS}(\rho,\tau)=\frac{1}{4\pi\rho\tau}\ln\left(\frac{\tau+\rho}{\tau-\rho}\right)$$

$$i_c^{SIS}(\tau)=\frac{1}{2\pi\tau^2}$$

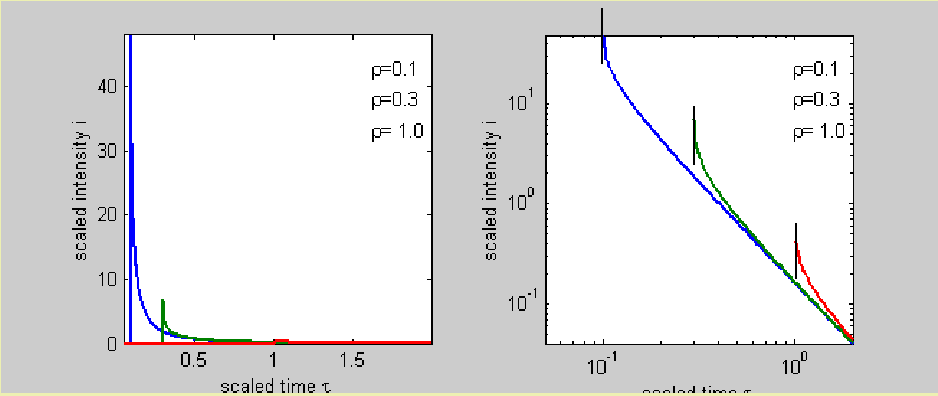

Main properties:

A. "positive" [fit regional waveforms]

1. Clear coda
2. Clear coda asymptote
3. Pulse envelope approaches coda asymptote from above

B. "negative" [contradict regional waveforms]

1. Spike-like arrival, no pulse broadening with distance
2. Inaccurate at ρ ≅ **1** or more

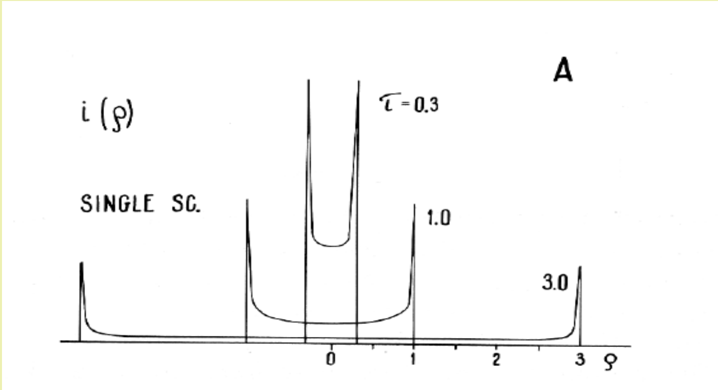

"Coda-Q" determination:

fit the observed coda shape selecting Q_C in the equation

$$I_c^{SIS}(t)=\frac{\exp(-2\pi ft/Q_C)}{2\pi clt^2}$$

Isotropic scattering case: diffusion approximation

τ » 1, any ρ

Diffusion isotropic scattering model – DIS

$$i^{\mathrm{DIS}}(\rho,\tau)=\frac{1}{(4/3\,\pi\tau)^{3/2}}\exp\left(-\frac{\rho^2}{4/3\,\tau}\right)$$

$$i_c^{\mathrm{DIS}}(\tau)=\frac{1}{(4/3\,\pi\tau)^{3/2}}$$

the solution of parabolic/diffusion equation for wave energy density $E(\mathbf{r},t)=P(\mathbf{r},t)/c$:

$$\partial E/\partial t = D\nabla^2 E$$

where $D=lc/3$ in 3-dim.case (or $lc/2$ *in* 2D)

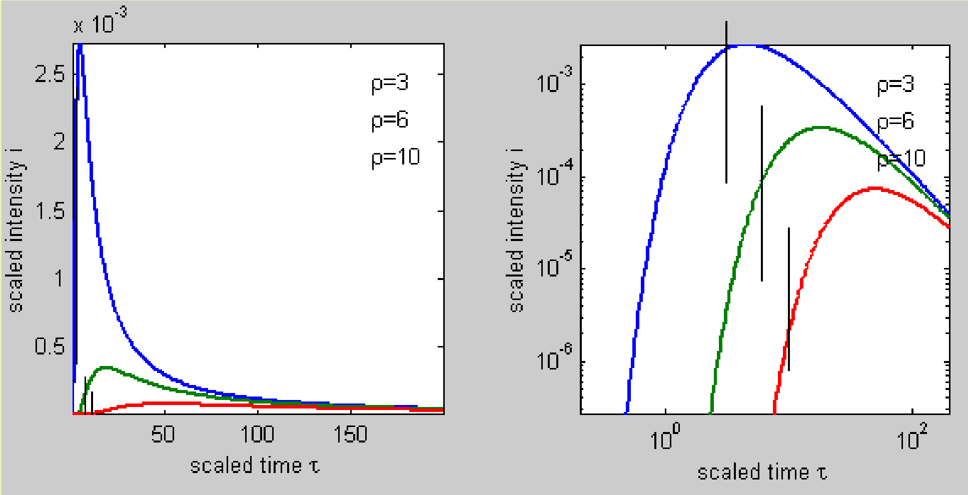

Main properties:

A. "positive" [fit regional waveforms]

1. Clear coda, clear coda asymptote
2. "Pulse" broadens with distance

B. "negative" [contradict regional waveforms]

1. "Pulse" envelope approaches coda asymptote from below
2. Weak arrival
3. "Pulse" is too long
4. In space, energy concentrates around the source
5. Bad model at ρ ≅ **2** or less

C. conclusion: Can fit lunar and volcanic data but not regional waveforms

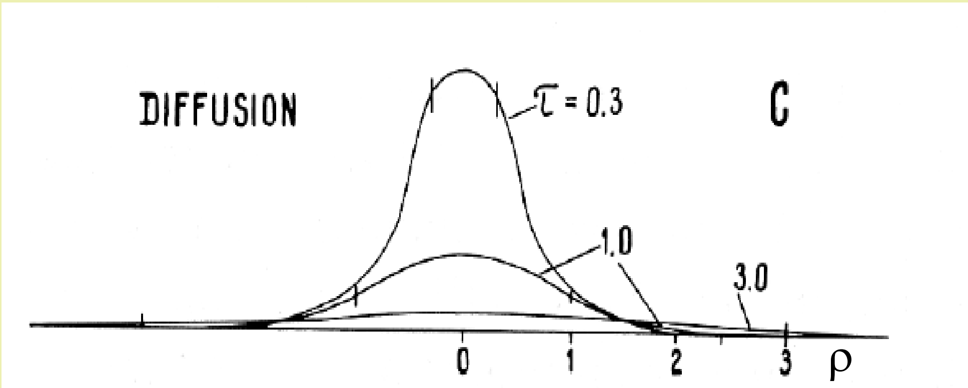

Isotropic scattering case: multiple

Multiple isotropic scattering model - MIS

any τ , any ρ

$$i^{\text{MIS}}(\rho,\tau) = << \begin{array}{c} \text{Numerical MC model (Gusev \& Abubakirov 1987)} \\ \text{Analytical series representation (Zeng et al. 1991)} \end{array} >>$$

$$i_c^{\text{MIS}}(\rho,\tau) \cong \frac{1}{2\pi\tau^2}\left[1+\left(\frac{27}{16\pi}\tau\right)^x\right]^{1/2x} \; ; \; x = 1.10 \quad \text{(Abubakirov \& Gusev 1990)}$$

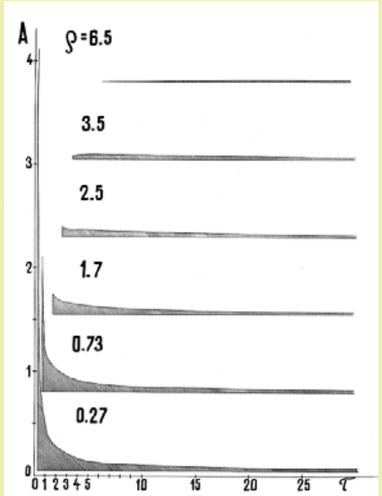

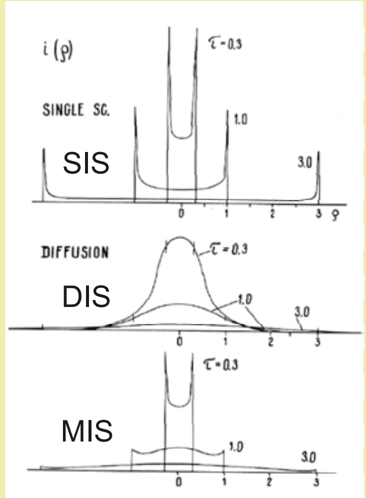

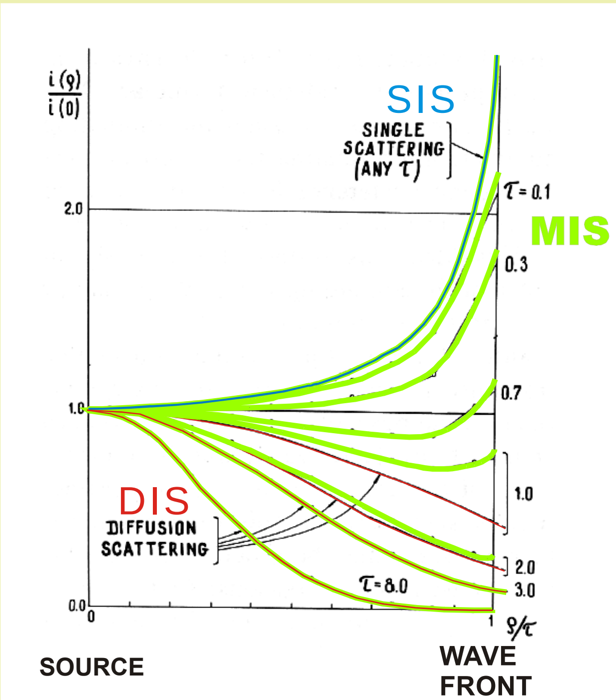

Main properties:

A. "positive" [fit regional waveforms]

1. Clear coda & coda asymptote

B. "negative" [contradict regional waveforms]

1. Spike-like arrival (or very long train):

    no realistic pulse broadening with distance

Multiple non-isotropic scattering

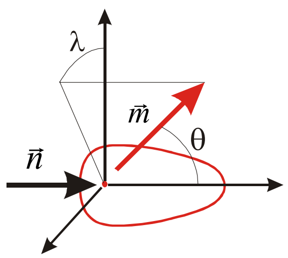

$\phi(\vec{n},\vec{m}) \Rightarrow \phi(\cos(\vec{n},\vec{m})) \Rightarrow \phi(\theta)$

non-isotropic, or anisotropic ("ray-anisotropic") case, axisymmetrical

("isotropic-medium" case, with statistically isotropic medium; no isotropy w.r.t. incident ray direction)

Instead of a single $l \equiv$MFP in the isotropic case, two characteristic lengths:

(1) l_n - "non-isotropic", "true" MFP,

(2) l - transport MFP, defined through diffusion asymptotics ($t \to \infty$) as $l=3D/c$ (in 3-dim.case)

dimensionless / scaled parameters:

$\rho \equiv r/l$	scaled distance ("transport")
$\tau \equiv cr/l = t/t^*$	scaled lapse time("transport")
$\rho_n \equiv r/l_n$	scaled distance ("common, true")
$\tau_n \equiv crt/l_n = t/t_n^*$	scaled lapse time ("common, true")
$i(\rho, \tau)$, $i_c(\tau)$	scaled scattered intensity (3D, use l^2 for 2D):

$$i(\rho,\tau) = i\left(\frac{r}{l}, \frac{t}{t^*}\right) = \left(\frac{l^3}{c}\right) P(r,t)$$

scaled coda intensity:

$$i_c(\tau) \equiv i(0,\tau)$$

MORE DEFINITIONS

basic parameters:

l, $t^* = l/c$, redefined as transport mean free path, and transport mean free time (compatible to previous definition)

l_n, $t_n^* = l_n/c$, (common) mean free path, and mean free time

Q transport quality factor due to scattering ($Q = \omega t^* = 2\pi l / \lambda$);

Q_n (common) quality factor due to scattering ($Q_n = \omega t_n^* = 2\pi l_n / \lambda$);

KEY FORMULA FOR TRANSPORT MFP

$$l = \frac{l_n}{1 - <\cos\theta>}$$

where

$$<\cos\theta> = \int_{4\pi} \phi(\Omega)\cos\theta \, d\Omega =$$

$$= \int_0^{\pi}\int_0^{2\pi} \phi'(\theta)\cos\theta\sin\theta \, d\lambda \, d\theta$$

Typical value for the Earth's lithosphere: $l \equiv$MFP=100 km, so for typical local/regional observations: ρ=0.3-2

Multiple low-angle scattering

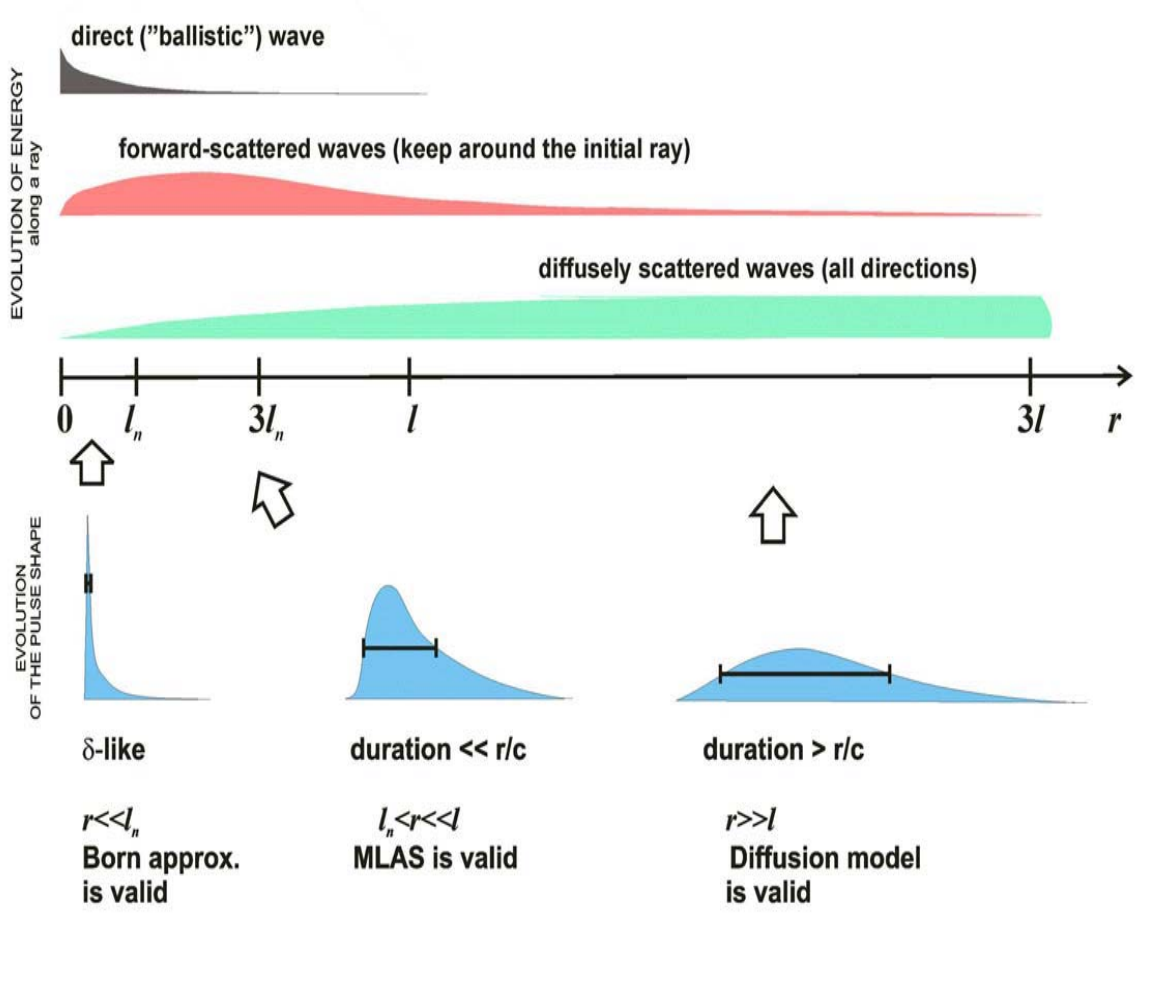

FORWARD-ENHANCED (NARROW) PHASE FUNCTION

$$<\theta^2> \ll 1$$

$$l_n / l = 1 - <\cos\theta> \approx <\theta^2>/2 \ll 1$$

DEFINITIONS

OF scattering-Q :

standard:

$$Q = 2\pi l_n / \lambda$$

(direct →

→ forward-scattered)

in seismology, in practice

$$Q = 2\pi l / \lambda$$

(direct +forward-scattered→

→diffusely-scattered)

[related to the habit to integrate entire "body-wave group" as *direct wave*]

Multiple low-angle scattering(2)

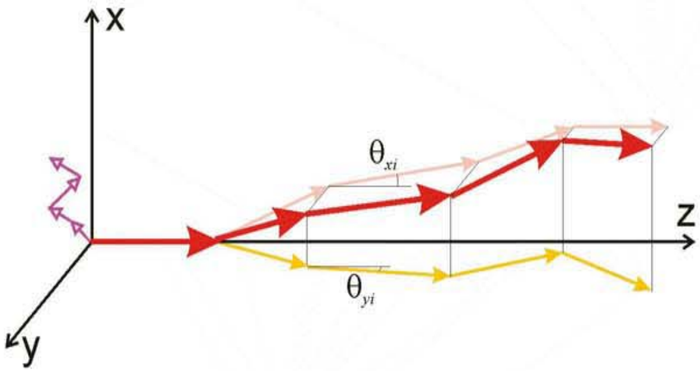

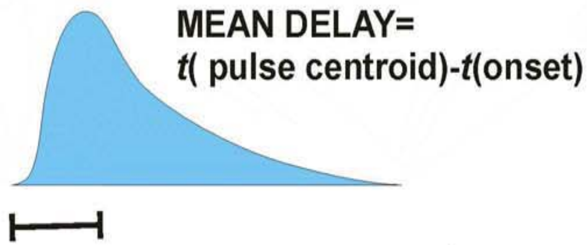

$$< T > = \int_{t_d}^{\infty} (t - t_d) E(t) dt \Big/ \int_{t_d}^{\infty} E(t) dt$$

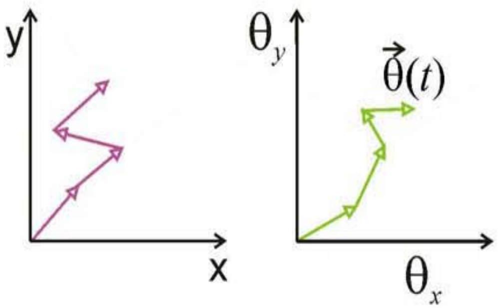

Assume

$<\theta_{xi}^2> \; < \; \infty$

$<\theta_{yi}^2> \; < \; \infty$

then $\vec{\theta}(t)$ is a Brownian motion

$$< T > = \frac{r^2}{6cl}$$

$$\tau_a = \frac{< T >}{t^*} = \frac{1}{6} \rho^2$$

Multiple non-isotropic scattering – simulation

Monte-Carlo simulation:
the standard technique
to solve real
radiative transport
problems.
No ready analytic solution
exists
for multiple non-isotropic
scattering
even in the case of
uniform-space geometry
and isotropic–medium
phase function

EXAMPLE
2D, τ=0.7, N=500
source:
needle-like radiation pattern
along +x

phase function:
isotropic

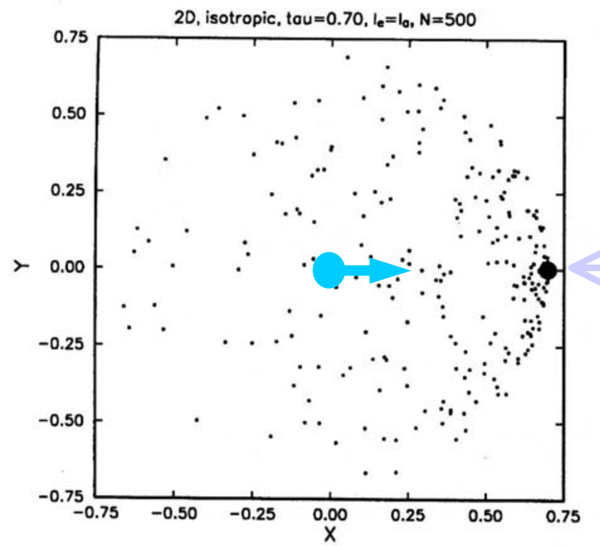

phase function:
$(\langle\theta^2\rangle)^{0.5}=\sigma=10^{o}$

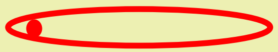

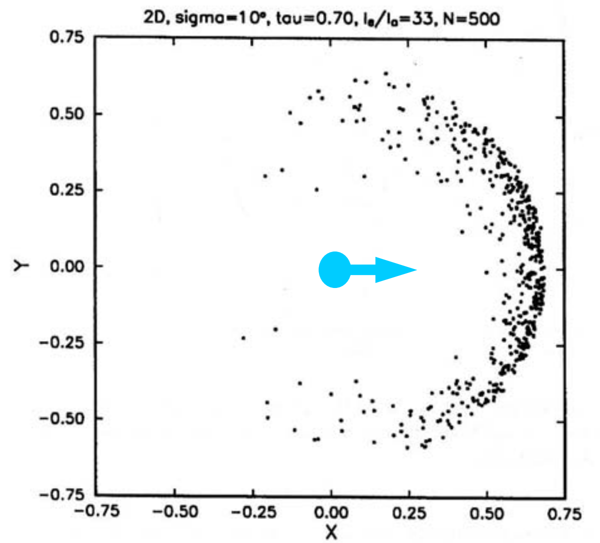

ballistic/direct component

Multiple non-isotropic scattering – simulated envelopes

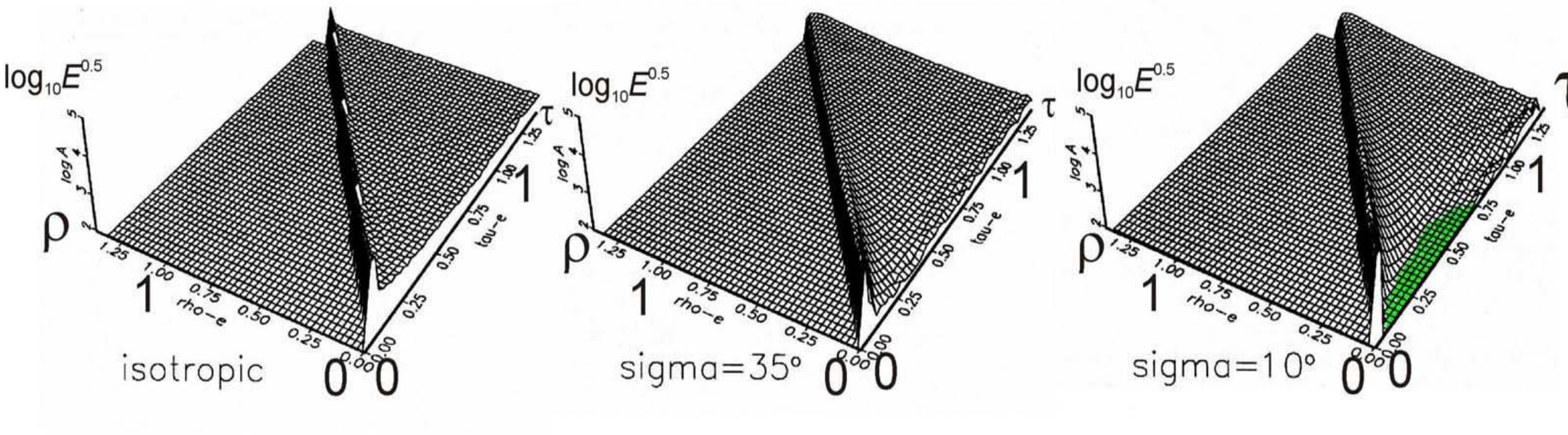

Isotropic scattering case:

spike-like energy pulse – no broadening, completely unrealistic

well-formed, monotonous, believable coda

Moderately elongated phase function (σ=35°):

acceptably broadening energy pulse

no minimum in coda, marginally acceptable

Narrow phase function (σ=10°):

well-formed, broadening energy pulse

coda with minimum, completely unrealistic

CONCLUSION: Both isotropic-scattering and MLAS models do not work. Real phase function must be moderately elongated

Which parameter specifies the scattering properties of the Earth's medium?

Three modes of analysis of observed signals are used to extract scattering properties of the Earth's medium:

(1) The ratio of coda amplitude to S-wave pulse amplitude
gives *l* - transport MFP

{traditionally, viewed at as "back-scattering MFP" or "isotropic-scattering MFP"}

[in an improved form, works as a part of MLTWA]

(2) The rate of S-wave pulse energy attenuation with distance
gives Q_{total} => *l* - transport MFP

{traditionally, the "scattering part" of Q_{total}^{-1} is treated as "the" scattering Q^{-1} and associated with "isotropic-scattering MFP"}

[in a modified form, works as a part of MLTWA]

(3) Pulse broadening rate with distance
gives *l* - transport MFP

No technique has been proposed in seismology to determine l_n- true MFP

and there are theoretical obstacles that complicate such a determination

A certain confusion is produced by using isotropic scattering model in the interpretation of observations

whereas in the Earth, the phase function is definitively forward-enhanced

In reality, most techniques that aimed at determination of MFP (or scattering *Q*), yield transport MFP

CONCLUSION:
one can continue to use the usual "seismological" scattering-*Q* parameter

but should keep in mind that it essentially related to transport MFP, and *not* to true MFP

Random inhomogeneity field and phase function

Random medium – the simplest case

(for the Earth, essentially, each assumption is an oversimplification)

Acoustic/scalar waves:

$$c(\boldsymbol{x}) = c_o(1+\varepsilon'(\boldsymbol{x}))$$

Weak inhomogeneity:
$\varepsilon'(\boldsymbol{x}) << 1$

Gaussian inhomogeneity - can be described by ACF:
$\mathrm{Cov}(\varepsilon'(\boldsymbol{x}), \varepsilon'(\boldsymbol{y}))$

Stationary inhomogeneity:
$\mathrm{Cov}(\varepsilon'(\boldsymbol{y}), \varepsilon'(\boldsymbol{y}+\boldsymbol{x})) = \sigma_\varepsilon^2 R'(\boldsymbol{x})$

Isotropic inhomogeneity:
$\mathrm{Cov}(\varepsilon'(\boldsymbol{y}), \varepsilon'(\boldsymbol{y}+\boldsymbol{x})) = \sigma_\varepsilon^2 R'(\boldsymbol{x}) = \sigma_\varepsilon^2 R(|\boldsymbol{x}|) = \sigma_\varepsilon^2 R'(r)$

Case	ACF	POWER SPECTRUM $k'=|\boldsymbol{k}'|$ is related to FT[$\varepsilon(\boldsymbol{x})$ of *medium*]	PHASE FUNCTION $k=|\boldsymbol{k}|=\omega/c$ is related to *propagating waves*
General	$R(r)$	$\tilde{R}(k')$	$\phi(\theta)\propto k^4\tilde{R}(2k\sin(\theta/2))$
Gaussian ACF	$\exp(-r^2/a^2)$	$\propto\exp\left(-(ka)^2/4\right)$	$\phi(\theta)=\dfrac{\exp((\cos\theta-1)/\sigma^2)}{2\pi\sigma^2(1-\exp(-2/\sigma^2))}$ *where* $\sigma^2=2/(ka)^2$
self-affine	diverges at $r=\infty$	$k^{-\alpha}$	$\propto(\sin(\theta/2))^{-\alpha}$ diverges at $\theta=0$
Von Karman	$\propto\left(\dfrac{r}{a}\right)^{\kappa}K_\kappa\left(\dfrac{r}{a}\right)$	$\propto\dfrac{1}{(1+a^2k^2)^{\kappa+3/2}}$ $\approx k^{-(2\kappa+3)}$ when $k>>1/a$	$\propto k^2(1+4a^2k^2\sin^2(\theta/2))^{-(\kappa+3/2)}$ $\approx\sin(\theta/2)^{-(2\kappa+3)}$ as $k>>1/a$ (i.e. at not very small θ)

Random inhomogeneity field: models

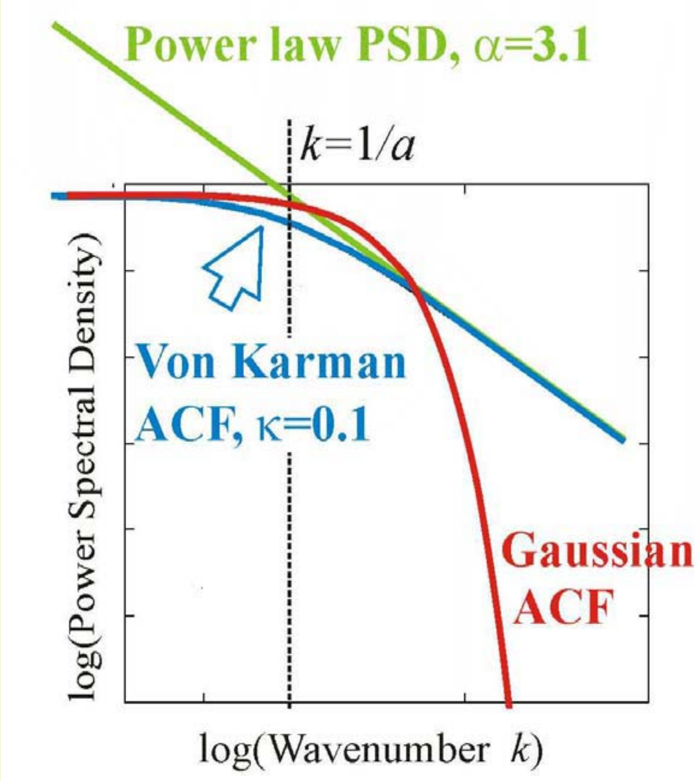

The case of self-similar inhomogeneity:
$\alpha=3$
$\kappa=0$

Case	**Properties of phase function $\phi(\theta)$ and power spectral density (PSD)**
Gaussian ACF:	$\phi(\theta)$: The angular width is strongly frequency-dependent: $\sigma = 2^{0.5}/ka$. PSD: Abrupt high-wavenumber cutoff
Self-affine case, power-law PSD:	$\phi(\theta)$: Frequency-independent shape for all θ PSD: *Non-integrable* (in practical calculation, PSD can be truncated at small k)
Von Karman ACF	$\phi(\theta)$: Through selecting a sufficiently large value of a, one can provide the frequency-independent behavior of $\phi(\theta)$ for almost all θ, except for very small θ ($<1/ka$). PSD: Integrable.

Models of random inhomogeneity field vs. reality

Case	**comments**
Gaussian ACF:	Qualitatively unacceptable model. The strong frequency dependence ($1/k \rightarrow 1/f$) of the width σ of phase function makes impossible to match the requirement: σ≈25-40° - simultaneously for many frequency bands.
Self-affine case, power-law PSD or Von Karman-ACF case with large ***a***	Qualitatively acceptable model. The frequency-independent shape of phase function for all or almost all angles enables one to fit the qualitative behavior of envelopes simultaneously for many frequency bands. [rough ranges for parameters: α=3.2-4; κ=0.1-0.5]

Simulated envelopes: Gaussian-ACF case

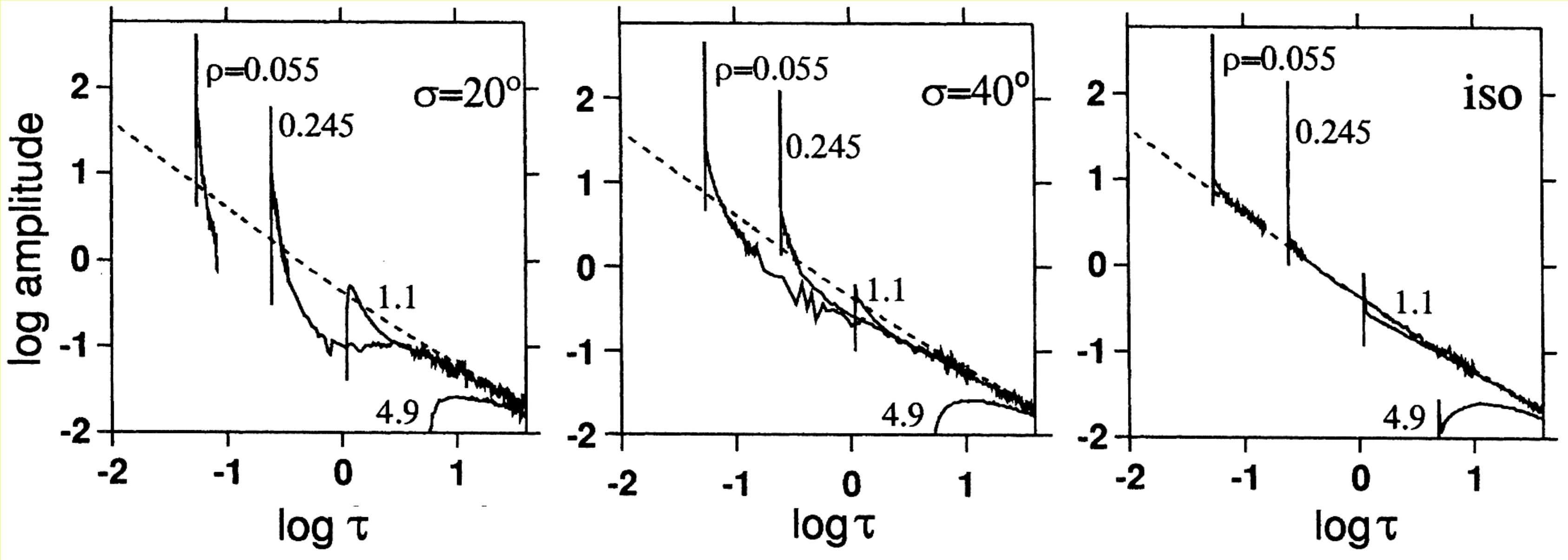

σ=20°
(1) gap instead of coda
(2) pulse broadens with distance

σ=40°
(1) acceptable coda, note that its level is below that for isotropic-scattering case
(2) spike instead of pulse up to ρ≈1.5

isotropic scattering **(σ=∞)**
(1) "perfect"coda
(2) no pulse broadening at all

The interval estimate for σ, namely σ =20-40°, is attained, but it works for a single frequency band only! Gaussian-ACF model is mostly of instructional interest!

Simulated envelopes: self-affine case

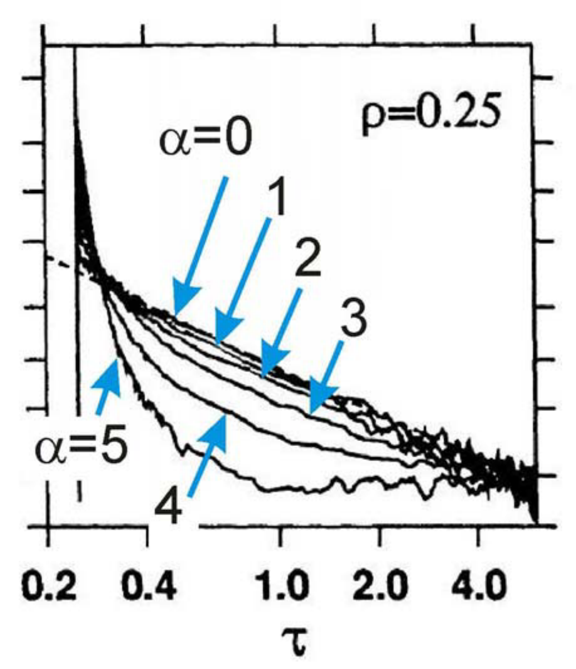

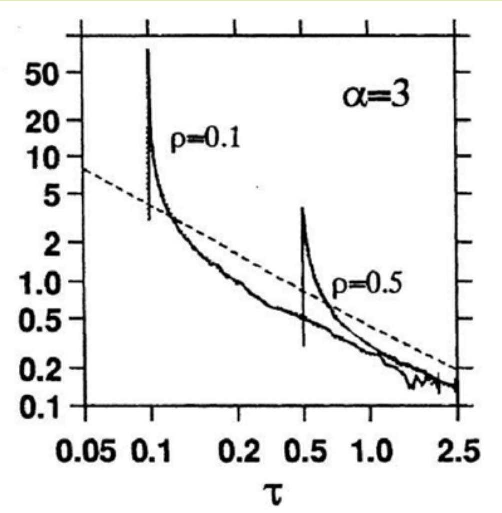

α=3

(1) quite acceptable coda shape

(2) slightly too abrupt pulse onset

α=4

(1) early coda somewhat too low

(2) acceptable pulse shape

CONCLUSION

(1) Self-similar random ihnomogeneity with α=3.2-4 is a reasonable starting model for the lithosphere

(2) Coda levels are systematically somewhat lower w.r.t. those of the isotropic scattering model (α=0)

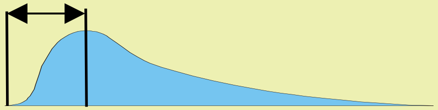

Duration of simulated envelopes

Scaled onset-to-peak delay time τ_m

vs. scaled distance ρ

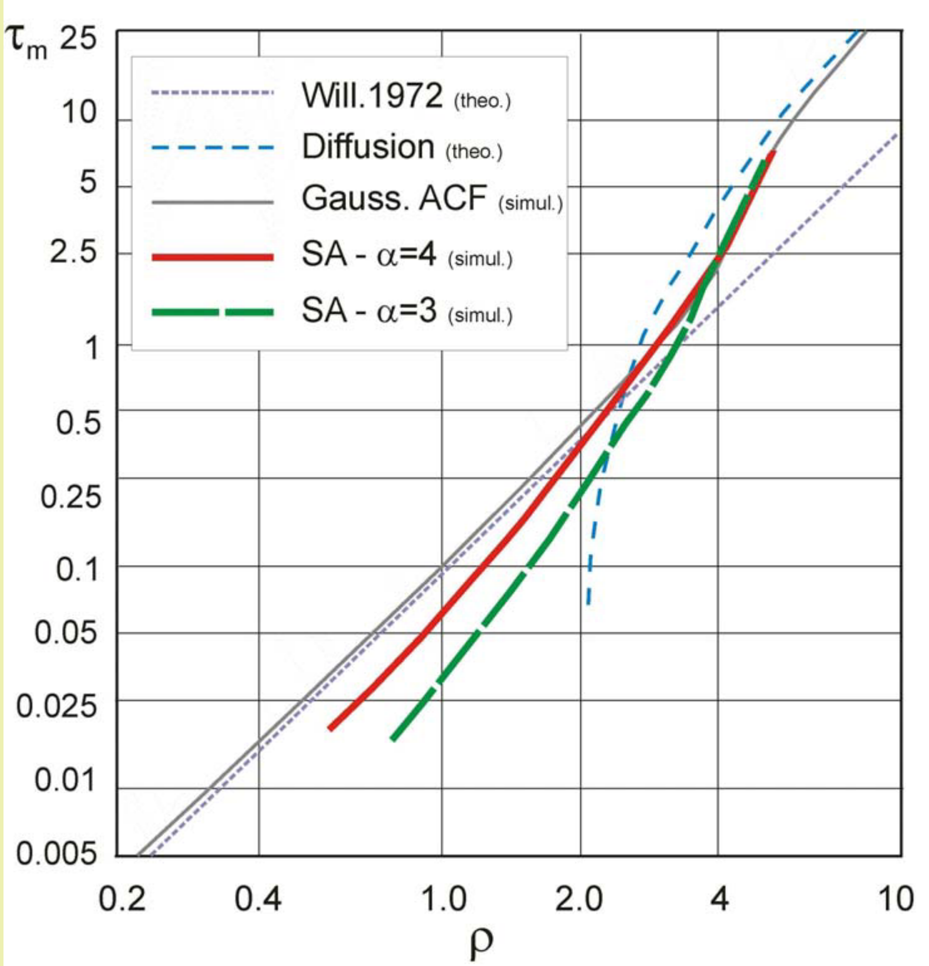

Gaussian-ACF case,
narrow phase function:

$$\tau_m = 0.091\rho^2$$

on condition $\rho \ll 1$
(Williamson 1972)

Onset-to-peak delay for a realistic self-similar medium is significantly *smaller* than for the Gaussian-ACF medium.

When the α parameter can be specified or assumed, one can use the results of Monte-Carlo simulation to derive l from the observed duration trend.

Ways for inversion for scattering/attenuation parameters (body waves)

approach	comment
A. Total attenuation Q^{-1}_{total} [$=Q^{-1}_{scattering}+Q^{-1}_{intrinsic}$] from body wave Fourier ***spectra***. A1. From spectra as is – one (or more) events at many stations. A2. From spectra normalized to coda power at one or more stations	Efficient descriptive approach, valid for eventual synthetics. Results physically not transparent. Systematic, consistent selection of the data window difficult. Using coda normalization significantly reduces noise.
B. Total attenuation Q^{-1}_{total} from body wave ***amplitudes***, raw or coda-normalized	Generally, outdated approach. Q^{-1}_{total} estimates often biased (because of variable, distance-dependent duration of the body wave group).
C. Separately $Q^{-1}_{scattering}$ *and* $Q^{-1}_{intrinsic}$ [add up to Q^{-1}_{total}] assuming isotropic scattering in uniform random meduim. C1. By MLTWA (Multiple Lapse-Time Window Analysis) method C2. From Pulse-energy to coda-power ratio at the same propagation time.	Consistent separate estimates of $Q^{-1}_{scattering}$ and $Q^{-1}_{intrinsic}$. Results may be significantly model-dependent

Ways for inversion for scattering/attenuation parameters (body waves) (2)

approach	comment
D. Only $Q^{-1}_{scattering}$ from body-wave pulse broadening.	Results may be model-dependent
E. Only $Q^{-1}_{intrinsic}$ from $\kappa(r)$ (κ in $A/A_o=\exp(-\pi\kappa f)$)	Efficient but works only for frequency-independent component of attenuation. May be biased by effects of source spectra
F. Determination of "coda Q"	The approach assumes single isotropic scattering i.e. an unrealistic model, and cannot yield reliable results; but supported by a number of empirical parallels between Q_{total} and coda Q. Empirical coda Q is often lapse-time dependent, but other Q measures may behave similarly.

MLTWA (after Fehler 2003)

Integrate Energy in Windows whose Times are Referenced to S-wave Arrival Time

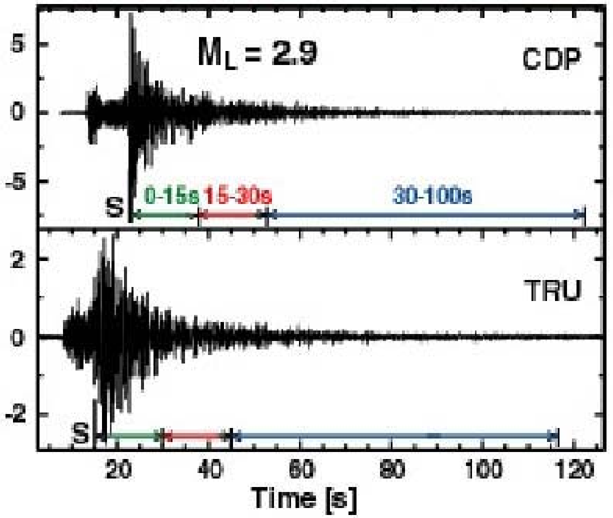

$$EI_1(f)_{kj} = \rho_0 \int_0^{15s} \left|\dot{u}_{kj}^S(t;f)\right|^2 dt,$$

$$EI_2(f)_{kj} = \rho_0 \int_{15s}^{30s} \left|\dot{u}_{kj}^S(t;f)\right|^2 dt,$$

$$EI_3(f)_{kj} = \rho_0 \int_{30s}^{100s} \left|\dot{u}_{kj}^S(t;f)\right|^2 dt$$

Results Obtained with Multiple Lapse-Time Window Analysis Method

Gives $g_0 \sim 0.01$ km^{-1}

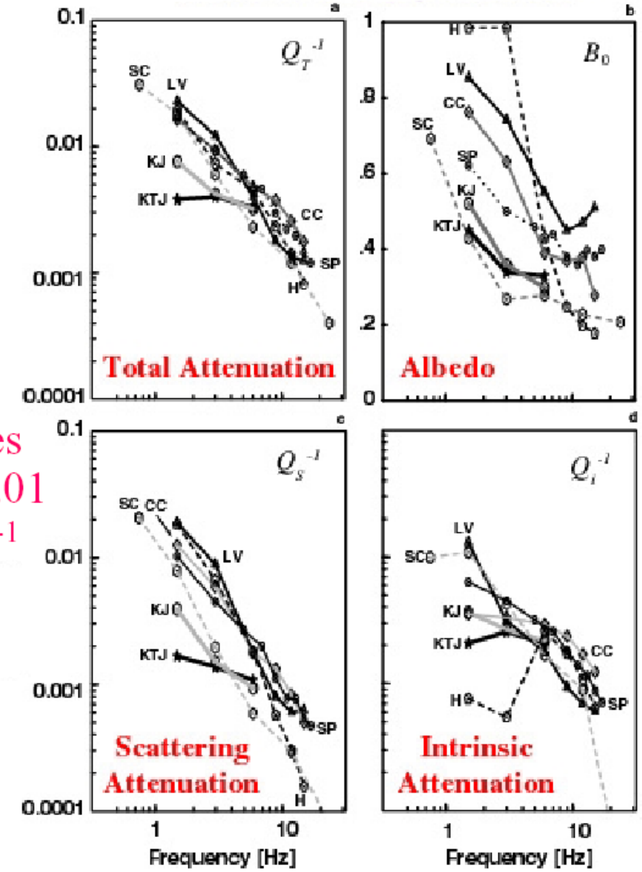

Fits to Data Collected in Japan

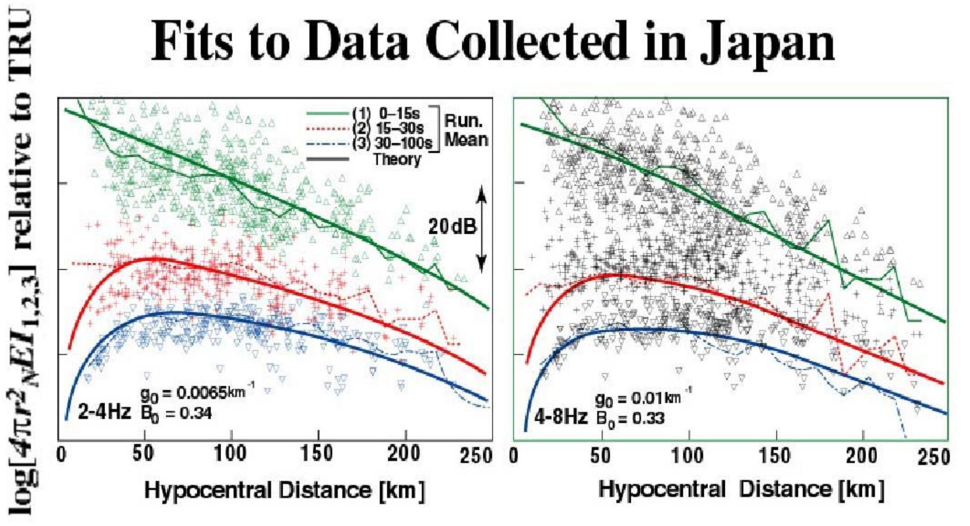

Scattering parameters from pulse duration vs distance trend

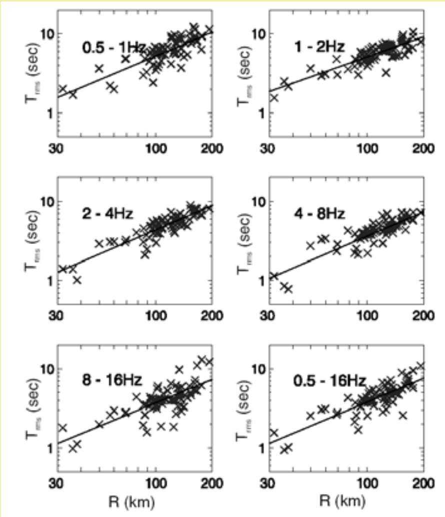

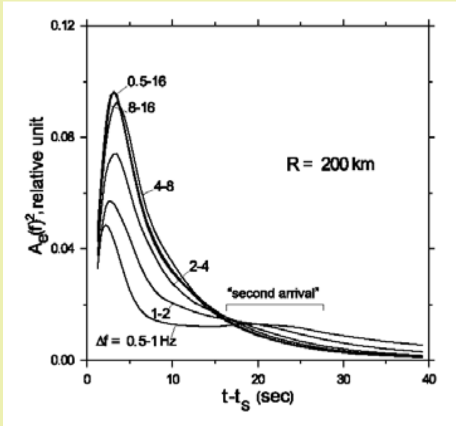

pulse shapes scaled along *t* axis, thus reduced to a fixed distance

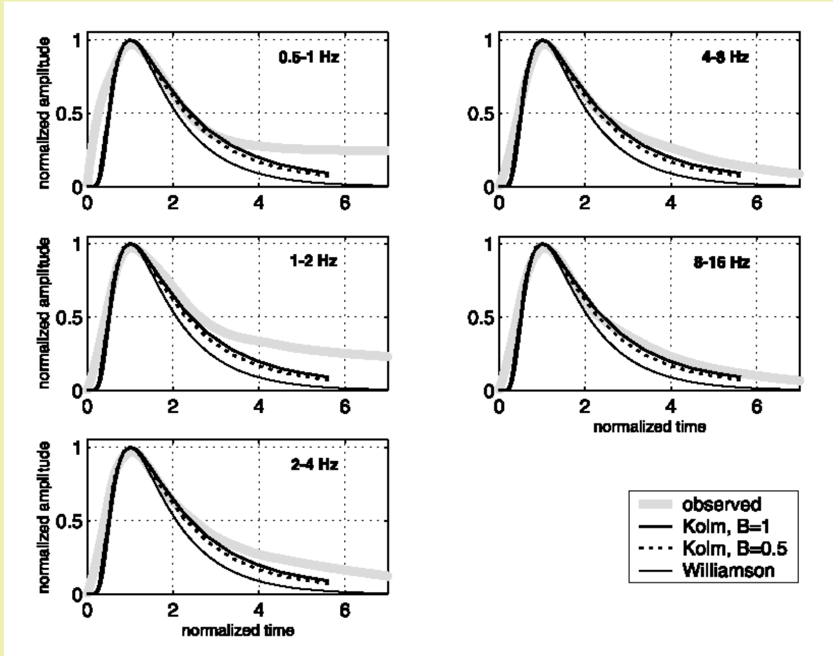

RMS duration of S-wave group for sta. PET grows as $r^{-1.0}$ indicating strongly distance-dependent scattering Q.
To determine MFP, onset-to-peak delays are used.
In the 1-12 Hz *f* range, and for *r*=100 km, MFP estimates are around 100km

Average pulse shapes and their fit by predictions of
(1) Gaussain-ACF model and
(2) self-similar inhomogeneity case with $\alpha=3\,^{2}/_{3}$ (Kolmogorov's spectrum)
The onset-to-peak delay vs frequency relationship indicates $\alpha\approx3.8$-3.9

Regional envelopes give qualitative understanding of scattering in the Earth(1)

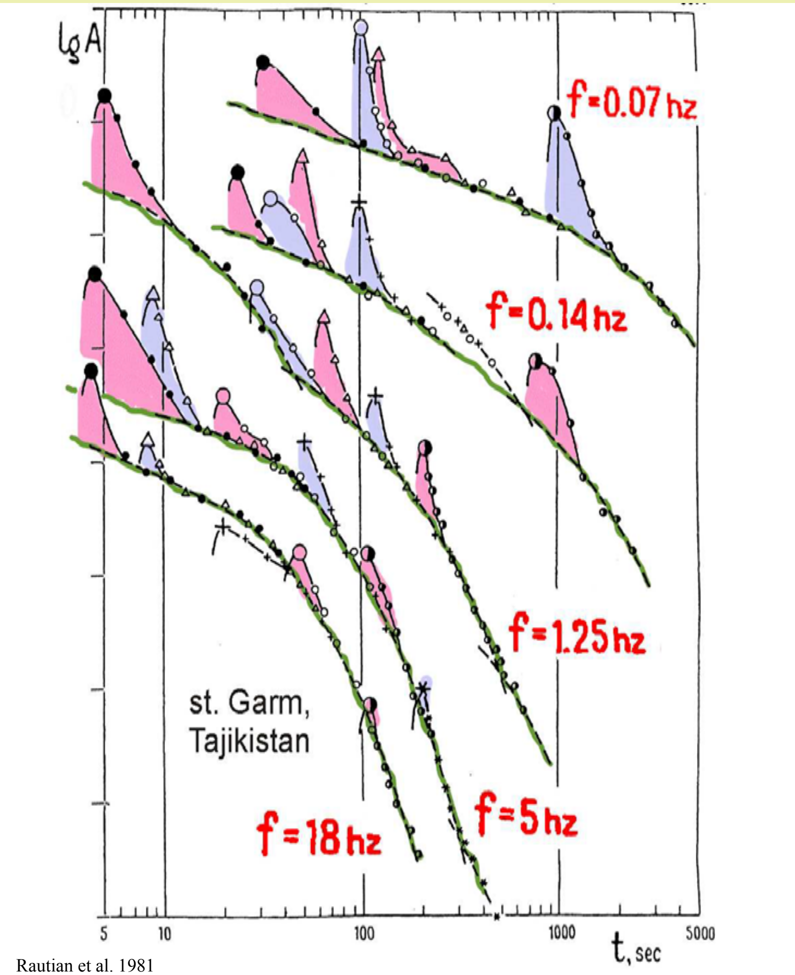

Rautian et al. 1981

(1) Over the entire 20-30 to 400-800 km distance range, the *S*-wave group/pulse is seen *above* coda asymptote.

(2) The duration of the pulse is increasing with distance. This pulse broadening is caused by medium, not source, and must be produced by forward-scattering. (Continental Lg is a special case).

(3)Diffusion scattering is not observed. Pulse duration is, roughly, proportional to distance.

(1,2,3) suggests scattering phenomena in general but do not match the picture of scattering in the uniformly scattering medium, (that predicts (a) quadratic trend of duration vs. distance, and (b) fast sinking of a pulse in the diffuse envelope)

All this implies: ***ray-average MFP is not constant but rapidly decreases with distance***.

Regional envelopes give qualitative understanding of scattering in the Earth(2)

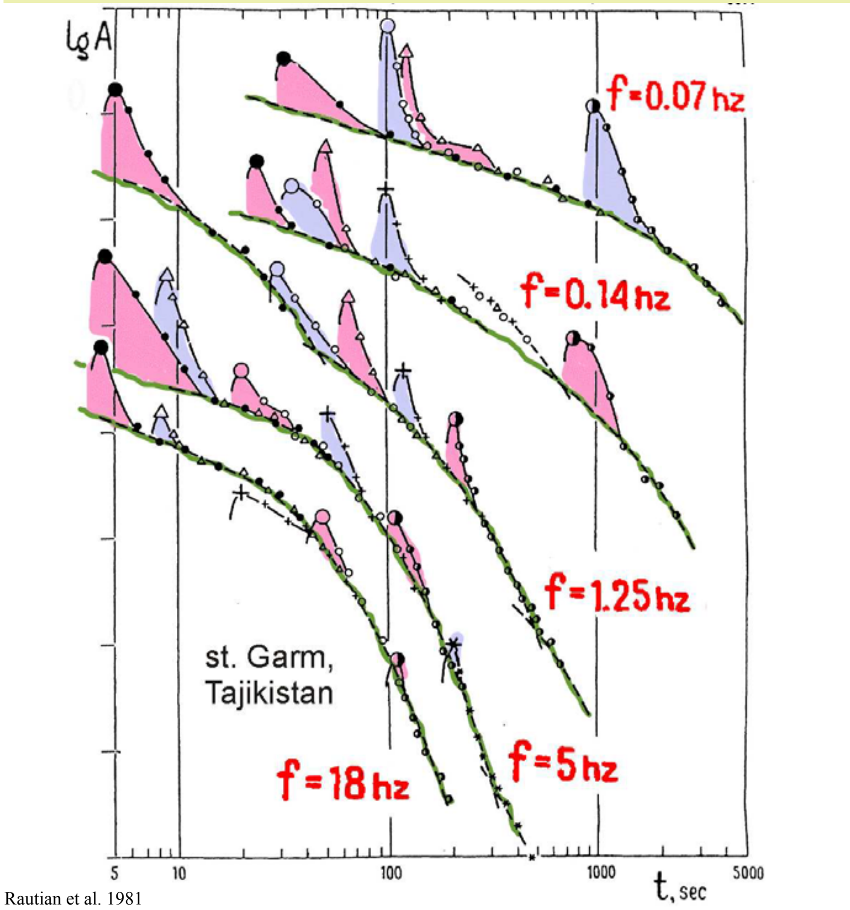

Rautian et al. 1981

Ray-average MFP is not constant but rapidly decreases with distance. Therefore, in the Earth, for almost any ray and any HF band:

distance ***r*** is less than or comparable to ray-average ***MFP***

or

ρ is less than or comparable to 1.0

As rays dive deeper with increasing distance, this means that in the Earth

scattering effects rapidly decay with depth

(follows as well from the existence of impulsive teleseismic P-waves)

Estimating the *transport MFP* vs. *depth* trend from coda shape

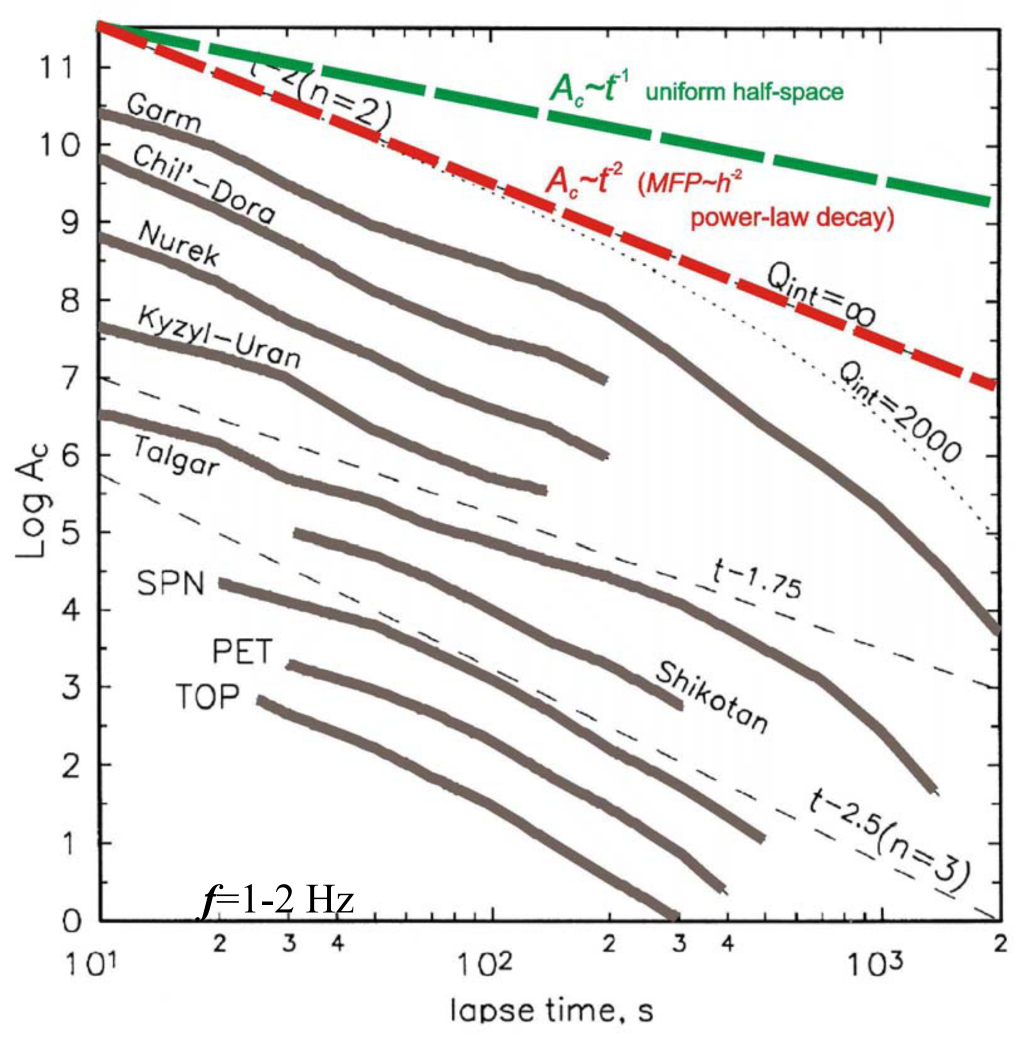

Observed coda amplitude over a wide lapse-time range follows neither

t^{-1} (SIS in the uniformly scattering space)

nor

$t^{-1} \exp(-\pi f t/Q_i)$

(same+intrinsic loss labeled "coda Q").

Instead, a trend like

$t^{-1.75\text{-}2.5}$

is seen,

corresponding to SIS in the scattering half-space with very fast depth decay of MFP:

$MFP(h) \sim h^{-1.5\text{-}3}$

(adjustment: $\exp(-\pi f t/Q_i)$ with Q_i=2000)

(A traditional coda-Q determination yields a mixture of MFP(h) effect and of intrinsic Q. It can match S-wave Q because a large fraction of S-wave attenuation is caused by radiation loss into deeper weakly scattering layers, thus emulating intrinsic loss in a uniform space.)

Estimating the *transport MFP* vs. *depth* trend from pulse broadening

Basis for inversion:

mean delay of a pulse = f ($g(\boldsymbol{r})$ along a ray)

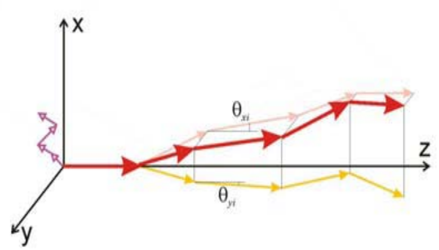

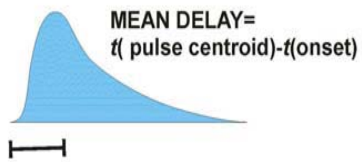

$$\langle T\rangle = \int_{t_d}^{\infty}(t-t_d)E(t)dt \Big/ \int_{t_d}^{\infty}E(t)dt$$

let transport MFP $l=l(\boldsymbol{r})$, tr. turbidity $g=1/l=g(\boldsymbol{r})$

(1) $g(\boldsymbol{r})=const=g$: $\langle T \rangle = \dfrac{g r^2}{6c}$ (Williamson 1972)

(2) non-uniform case: $\langle T \rangle = \dfrac{1}{cS}\displaystyle\int_0^S g(u)(S-u)u\,du$

where u is the along-ray distance and S is the length of the ray (Bocharov 1988)

in practical inversion assuming α=3.7 and thus: onset-to-peak delay =0.28<*T*>

inverted vertical profiles $g(h)$ for *P* and *S* waves under Kamchatka (based on ~2500 onset-to-peak delays, from hypocenters at *h*=20-300 km)

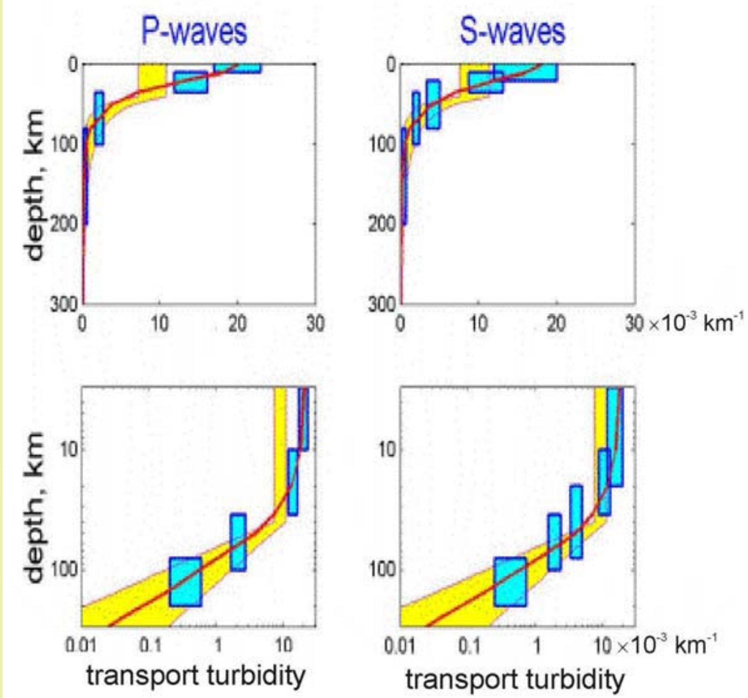

colors: different estimates

1. from *h*=10-15 to *h*=40-50 km: TMFP ~ 50-100 km
2. from h=60-80 km down, fast decay: TMFP ~ $h^{-2\text{-}3}$

VERY IMPORTANT TOPICS NOT COVERED:

1. Conversion scattering: P→S, S→P, S→surface wave ...)
2. Surface wave (2D) scattering.
3. Inversion of the HF radiation capability function (seismic luminosity) of a finite earthquake source from scattered envelopes

OTHER IMPORTANT TOPICS NOT COVERED :

1. Regional specificity of scattering. Case of Lg
2. Inversion of diffusive envelopes.
3. Synthesis of scattered envelopes.
4. Inversion of observed coda for the relative density of scatterers in 2D or 3D (assuming uniform Q)
5. Inversion of observed coda for the distribution of Q (assuming uniform density of scatterers)
6. Diffraction-based approach (Flatte&Wu 1988)

Reading/key references

Abubakirov, I. R. and A. A. Gusev, Estimation of scattering properties of lithosphere of Kamchatka based on Monte-Carlo simulation of record envelope of a near earthquake. Phys. Earth. Planet Inte-riors, 64, 52-67, 1990

Aki, K. and B. Chouet, 1975, Origin of coda waves: source, attenuation and scattering effects, J.Geophys. Res., 80, 3322-3342.

Aki, K., and B. Chouet, Origin of coda waves: source, attenuation and scattering effects, J. Geophys. Res. 80, 3322-3342. 1975.

Aki. K. Scattering of P-waves under Montana LASA. J.Geophys. Res. 78, 1334-1346, 1973.

Bocharov A.A. Mean delay and broadening of a pulse produced by scattering in the random inhomogeneous medium. Izv.vuzov, Radiofizika, 1988, v31, #11, pp1407-1409. (in Russian)

Dainty A.M.and M.N.Toksoz. 1977 Elastic wave propagation in a highly scattering medium_ Journal of Geophysics 43: 375-388

Dainty, A. M., A scattering model to explain seismic Q observa-tions in the lithosphere between 1 and 30 Hz. Geophys. Res. Lett., 8, 1126-1128, 1981.

Fehler, M., H. Sato and L-J, Huang, 2000, Envelope broadening of outgoing waves in 2-D random media: A comparison between the Markov approximation and numerical simulations,Bull. Seismol. Soc. Amer., 90, 914-928.

Fehler, M., Hoshiba, M., Sato, H., and Obara, K. (1992). Separation of scatteringand intrinsic attenuation for the Kanto-Tokai region, Japan, using measurements of S-wave energy versus hypocentral distance, Geophys. J.Int. 108, 787–800.

Flatté , S.M. and R.-S. Wu, Small-scale structure in the lithosphere and astenosphere deduced from arrival time and amplitude fluctuations at NORSAR. J.Geophys. Res. 93, 6601-6614. 1988.

Gusev A. A. and I. R. Abubakirov. Simulated envelopes of non-isotropically scattered body waves as compared to observed ones: another manifestation of fractal inhomoheneity. Geophys. J.Int. 127, 1996b, 49-60.

Gusev A.A. , and V.M.Pavlov. Deconvolution of squared velocity waveform as applied to study of non-coherent short-period radiatorin earthquake source. Pure Appl. Geophys 1991, 136: 235-244

Gusev A.A., Temporal variations of the coda decay rate on Kamchatka: are they real and precursory? J.Geophys. Res.102, 8381-8396, 1997

Gusev A.A.. Bay-like and permanent variations of the relative level of the late coda during 24 years of observation on Kamchatka. 1995.J.Geophys.Res., v100 N B10 pp 20311-20319

Gusev, A. A., and I. R. Abubakirov, Monte-Carlo simulation of record envelope of a near earthquake. Phys. Earth. Planet Interiors, 49, 30-36, 1987.

Gusev, A. A., and V. K. Lemzikov.Properties of scattered elastic waves in the lithosphere of Kamchatka: parameters and temporal variations, Tectonophys., 112, 137-153. 1985

Gusev, A.A., Vertical profile of turbidity and coda Q, Geophys. J. Int.,123, 665-672, 1995.

Ishimaru, A. Wave propagation and scattering in random media, vol. 1 and 2, 572pp, Academic, San Diego, Calif., 1978.

Ishimaru, A., 1978, Wave propagation and scattering in random media, Vols. 1 and 2, Academic Press, New York.

Kakehi, Y. and Irikura, K. (1996). Estimation of high-frequency wave radiation areas on the fault plane by the envelope inversion of acceleration

Kopnichev, Yu. F., Short-period seismic wavefields. Nauka, Moscow, 1985, 176pp. (in Russian).

Leary, P., Igel, H., Mora, P., and Rodrigues, D. (1993), Finite-di.erence Simulation of Trapped Wave Propagation in Fracture Anisotropic Low-velocity Layers, Can. J. Explor. Geophys. 29, 31–40.

Malin, P. E. (1980), A First-order Scattering Solution for Modeling Elastic Wave Codas; I. The Acoustic Case, Geophys. J. Roy. Astron. Soc. 63, 361–380.

Mitchell, B. J., Xie, Y.-P. J., and Cong, L. (1997). Lg coda Q variation acrossEurasia and its relation to crustal evolution, J. Geophys. Res., 102, 22767-22779.

More reading/references

Nishigami, K. (1991). A new inversion method of coda waveforms to determine spatial distribution of coda scatterers in the crust and uppermost mantle, Geophys. Res. Lett. 18, 2225–2228.
Obara, K., and Sato, H. (1995). Regional differences of random inhomogeneities around the volcanic front in the Kanto-Tokai area, Japan, revealed from the broadening of S wave seismogram envelopes, J. Geophys. Res. 100, 2103–2121.
Petukhin A.G. and A.A.Gusev. 2003. The duration-distance relationship and average envelope shapes of small Kamchatka earthquakes. Pure appl. geophys. 160 1717 –1743.
Rautian, T. G., and Khalturin, V. I. (1978). The use of the coda for determination of the earthquake source spectrum, Bull. Seismol. Soc. Am. 68, 923–948.
Rautian, T. G., V. I. Khalturin, M. S. Zakirov, A. G. Zemtsova, A. P. Proscurin, B. G. Pustovitenko, A. N. Pustovitenko, L. G. Sinelnikova, A. G. Filina and I. S. Shengelia. Experimental studies of seismic coda. Nauka, Moscow, 142pp. 1981. (in Russian)
Revenaugh, J. (1995). The contribution of topographic scattering to teleseismic coda in Southern California, Geophys. Res. Lett., 22, 543-546.
Rytov, S.M, Yu.A. Kravtsov and V.I.Tatarskii. Introduction to statistical radiophysics, Vol.1-4, Springer, New York 1987
Ryzhik, L. V., G. C. Papanicolaou and J. B. Keller, 1996, Transport equations for elastic and other waves in random media, Wave Motion, 24, 327-370.
Sato H. Mean free path of S-waves under the Kanto district of Japan. J. Phys. Earth. 1978. V. 26. P. 185-198.
Sato, H. (1984). Attenuation and envelope formation of three-component seismograms of small local earthquakes in randomly inhomogeneous lithosphere, J. Geophys. Res. 89, 1221–1241.
Sato, H., and Fehler, M. (1998). “Seismic Wave Propagation and Scattering in the Heterogeneous Earth”, AIP Preess/ Springer Verlag, New York.
Sato, H., Unified approach to amplitude attenuation and coda excitation in the randomly inhomogeneous lithosphere. Pure Appl.Geophys. 132, 93-119, 1990. seismograms, Geophys. J. Int. 125, 892–900.
Tsujiura, M. (1978). Spectral analysis of the coda waves from local earthquakes, Bull. Earthq. Inst. Univ. Tokyo 53, 1–48.
Wagner GS. 1996. Numerical simulation of wave propagation in heterogeneous wave guides with implications for regional wave propagation and the nature of lithospheric heterogeneity. Bull. Seismol. Soc. Am.96:1200–1206
Williamson, I. P., Pulse broadening due to multiple scattering in the interstellar medium. Mon. Not. R. astr. Soc. 157, 55-71, 1972.
Wu, R.-S. and Aki, K. (1985), The Fractal Nature of the Inhomogenneities in the Lithosphere Evidenced from Seismic Wave Scattering, Pure Appl. Geophys. 123, 805–818.
Wu, R.-S., and Aki, K. (1985). Elastic wave scattering by random medium and the small-scale inhomogeneities in the lithosphere, J. Geophys. Res. 90, 10261-10273.
Xie, J., and B. J. Mitchell, A back-projection method for imaging large-scale lateral variations of Lg coda Q with application to continental Africa, Geophys. J. Int., 100, 161-181, 1990.
Zeng, Y., Su, F., and Aki, K. (1991). Scattering wave energy propagation in a random isotropic scattering medium 1. Theory, J. Geophys. Res. 96, 607–619.

The sources of some graphics above:
H.Sato. http://www.zisin.geophys.tohoku.ac.jp/~sato/lecturenotes/SatoSeismWaveScat110201.pdf
M.Fehler. http://www.ees4.lanl.gov/staff/fehler/Fehler_MGSS_Talk_1.pdf
M.Fehler. http://www.ees4.lanl.gov/staff/fehler/Fehler_MGSS_Talk_2_part_1.pdf

More complete references see at: http://www.scat.geophys.tohoku.ac.jp/